Universidade do Minho
Escola de Engenharia

Sara Cristina Ribeiro Grincho Pinela

Evaluation of Nanoporous Materials for Biotoxin Capture

Dissertação de Mestrado

Mestrado Integrado em Engenharia Biológica

Ramo de Tecnologia do Ambiente

Trabalho efetuado sob a orientação do(s)

Professor João Peixoto

Doutora Begoña Espiña

Doutora Laura Salonen

setembro de 2016

DECLARAÇÃO

Nome: Sara Cristina Ribeiro Grincho Pinela

Título da dissertação: Evaluation of Nanoporous Materials for Biotoxin Capture

Orientador(es):

Professor João Peixoto

Doutora Begoña Espiña

Doutora Laura M. Salonen

Ano de conclusão: 2016

Designação do Mestrado: Mestrado Integrado em Engenharia Biológica – Ramo de Tecnologia do Ambiente.

Universidade do Minho, ___/___/_____

Assinatura:

ACKNOWLEDGMENTS

As I reach the end of my course, I can't let it pass without thanking all the people who have crossed my path during the last few years.

In particularly, I'd like to thank to my INL's supervisor, Dr. Begoña Espiña, for all the help, patience, availability and support she has been granting to me these past six months. To my INL's co-supervisor, Dr. Laura Salonen, for always having the time for me, and for all the support. I also want to thank to Soraia and João, for being the best COFs makers I've ever known. To my UM supervisor, Professor João Peixoto, for clarifying all of my doubts, for the support he has shown to my work and the time he has taken explaining to me, some of the mistakes that, without him, I wouldn't have known I had made.

I also need to thank my Mother, Augusta, for everything she did for me, since the day I was born, and for being my rock. To my grandmother, Iriete, and to my grandfather, Rogério, for always been there for me. To Pedro for all the patience during the past months, and all the love in past four years. To my Aunts and Uncles, Marília, Jorge, Helena, Sandra, Fernando, Andreia and Manel, for the support. A special thank you to Uncle João, for all the times in my life where he was more like a big brother to me than an Uncle, and to my Uncle and Godfather, Paulo, for the linguistic corrections and support. To my little cousins, Jéssica, Daniela, Ana Patrícia, Lara and Ema for never let me forget the child in me. To Fernando and Sílvia for being the best cousins to grow up with.

To Cátia, for being the best friend a girl can have. To my course mates, in special to Fátima, Daniela, Andreia, and Teresa for making these college years truly amazing and worthwhile.

To all people in INL who have received me so well and were always so supportive, in special to the people in Food and Environment Group. A special thank you to Marília, Marisa, Vânia, Marina, Liliana and Fátima for being awesome labmates.

At last, I want to thank all of my friends for the support they have shown me. To my High School teachers, for transmitting me the love for science and to my college Professors, for the knowledge I have acquired in the last years.

RESUMO

As biotoxinas são metabolitos produzidos por algumas espécies de microalgas, que podem atingir altas concentrações aquando uma proliferação maciça das mesmas ocorre. Este tipo de compostos é especialmente perigoso quando concentrados nos sistemas digestivos do marisco. Geralmente, as biotoxinas não afetam o marisco, porém, a sua presença torna-o impróprio para consumo humano. Neste sentido, é importante que se melhorem os métodos de monotorização de biotoxinas na água, de maneira a que se possa estabelecer um sistema de alerta antecipado, antes de o marisco se tornar tóxico.

Esta dissertação propõe um aperfeiçoamento de dispositivos de Solid Phase Adsorption Toxin Tracking (SPATT), para uma deteção atempada da presença de biotoxinas na água. Para tal, em vez das resinas geralmente usadas nos dispositivos SPATT, foi avaliado um novo material nanoporoso, Covalent Organic Frameworks (COFs), devido à uniformidade do tamanho de poro deste material ser mais semelhante ao tamanho das toxinas.

Testes de adsorção/desorção da toxina lipofílica ácido ocadaíco (OA) foram feitos, à escala laboratorial, assim como testes de reuso do material adsorvente. As cinéticas de adsorção e a isotérmica de adsorção a 19 °C foram determinadas. Por fim, a difusão da toxina nos poros do COF foi outro ponto estudado.

Os resultados dos testes laboratoriais realizados mostram que os COFs podem melhorar o desempenho dos dispositivos de SPATT, uma vez que conseguem capturar muito mais quantidade de toxina (cerca de 30 vezes mais) que as resinas geralmente usadas nos dispositivos de SPATT e conseguem fazê-lo muito mais rapidamente, devido ao facto de a difusão da toxina nos poros ser quase instantânea. A isotérmica de Freundlich determinada mostrou ter uma tendência linear favorável. Por fim, o COF pode também ser reutilizado, uma vez que a dessorção de toxina pode ser feita com sucesso, usando solventes orgânicos, como o etanol a 70 % e o acetonitrilo.

PALAVRAS-CHAVE

Ácido Ocadaíco, Malhas Orgânicas com ligações Covalentes, Proliferações de Algas Perigosas, Rastreamento de Toxinas por Adsorção em Fase Sólida

ABSTRACT

Biotoxins are metabolites produced by some microalgae species that can reach high concentrations when a massive proliferation of them occur. These kind of compounds are especially dangerous when concentrated in digestive glands of seafood. In general, biotoxins do not affect mollusks, however, the presence of biotoxins turns the mollusks unappropriated for human consumption. In this way, it is very important to improve monitoring methods of biotoxins in water in order to generate an early warning system before seafood becomes toxic.

This thesis proposes an improvement in Solid Phase Adsorption Toxin Tracking (SPATT) devices for early warning of the presence of biotoxins in water. To do so, instead of using the chromatographic resins commonly used in SPATT devices, a new nanoporous material, Covalent Organic Frameworks (COFs), was evaluated due to their pore uniform size to be similar to the toxins size.

Adsorption/desorption tests of the lipophilic toxin okadaic acid (OA) in COFs were performed, at laboratorial scale, as well as tests of the reuse of the adsorbent material. Adsorption kinetics and adsorption isotherm at 19 °C were determinated. Finally, diffusion of the toxin into the pores was studied.

The results showed that COFs could improve SPATT devices performance since they can capture much more quantity of toxin (about 30 times more) that common chromatographic resins and faster due to the fact that toxin diffusion in pores is almost instantaneous. The determined Freundlich isotherm showed a favorable linear tendency. Finally, COFs can be reused, once desorption can be successfully made using solvents, such as 70 % ethanol and acetonitrile.

KEYWORDS

Okadaic Acid, Covalent Organic Frameworks, Harmful Algae Blooms, Solid Phase Adsorption Toxin Tracking (SPATT).

INDEX

FIGURE INDEX

TABLE INDEX

LIST OF ABBREVIATIONS, INITIALS AND ACRONYMS

APS – Amnesic Shellfish Poisoning

AZP – Azaspiracid Shellfish Poisoning

BET – Brunauer-Emmett-Teller Method

c – concentration

CE – Capillary Electrophoresis

C_e – equilibrium concentration of the solute in solution

COF – Covalent Organic Framework

d_p – Pore diameter

D_{ef} – Coefficient of Effective Diffusivity,

D_m – Coefficient of Molecular Diffusivity

DiFMUP – 6, 8-difluoro-4-methylumbelliferyl phosphate

DPS – Diarrhetic Shellfish Poisoning

DTX1 – Dinophysistoxin-1

DTX2 – Dinophysistoxin-2

DTX3 – Dinophysistoxin-3

ELISA – Enzyme-linked Immunosorbent Assay

ESP – Environmental Sample Processors

FISH – Fluorescence *in situ* Hybridization

HAB – Harmful Algal Bloom

HPLC – High Performance Liquid Chromatography

IC_{50} – concentration of a compound needed to inhibit a biological or biochemical function in 50 %

IPMA – Instituto Português do Mar e da Atmosfera

LC-FD – Liquid Chromatography with Fluorescence Detection

LC-MS – Liquid Chromatography with Mass Spectrometry

M – Molecular Weight

MBA – Mouse Bioassay

MU – Mouse Unit

NSP – Neurotoxic Shellfish Poisoning

OA – Okadaic Acid

PC – Percentage of okadaic acid capture in adsorption assays

PR – Percentage of okadaic acid recovered in desorption assays

PP-1 – Protein Phosphatase-1

PP-2A – Protein Phosphatase-2A

PP-3 – Protein Phosphatase-3

PP-4 – Protein Phosphatase-4

PSP – Paralytic Shellfish Poisoning

q – quantity of solute which is adsorbed per quantity of adsorbent

q_e – quantity of solute adsorbed in equilibrium

q_t – quantity of solute adsorbed in each instant

q_m – maximum quantity of solute adsorbed

S – Surface Area

SAXS – Small Angle X-Ray Spectroscopy

SPATT – Solid Phase Adsorption Toxin Tracking

STX – Saxitoxin

S.W. – Sea Water

T – Temperature

t – Time

V_m – Molar Volume

ε – Porosity

μ – Viscosity

τ – Tortuosity

1. INTRODUCTION

1.1. General Background

Massive proliferation of microalgae or Harmful Algal Blooms (HABs) are phenomena that occur naturally. However, their frequency and intensity has increased in the last decades. When microalgae species are biotoxin producers, these phenomena are called toxic HABs. The consequent release of the biotoxins to the aquatic environment is particularly dangerous (NOAA, 2016).

The biotoxins present in the aquatic environment can be concentrated, particularly, in the digestive glands of shellfish, such as mussels, scallops, oysters and clams. Although those compounds are in general not toxic to shellfish, they are toxic for the human consuming them, leading to intoxications. This represents a problem of public health (Scoging, 1998).

The current law (Regulation (EC) No 853/2004 laying down specific hygiene rules for food of animal origin) does not allow the commercialization of the shellfish with levels of toxins higher than the regulatory limits established by the same law. However, the interdictions to aquaculture industries are only imposed when the shellfish are already improper for human consumption. This happens because the detection and quantification methods for biotoxins are applied to the shellfish itself. This fact leads to losses for aquaculture industries.

According to data from Instituto Português do Mar e da Atmosfera (IPMA), in Portugal, the major interdictions imposed to the aquaculture are due to the presence of lipophilic biotoxins, such as okadaic acid and its analogues. The interdiction periods can reach even six months per year (IPMA, 2016).

Consequently, there is a necessity of creating a mechanism that allows for detecting increasing concentrations of biotoxin before the shellfish becomes toxic. Due to the low concentrations of the biotoxins in water in the beginning of a HAB, they need to be concentrated in order to be quantified by the existing detection methods.

In 2004, MacKenzie and co-workers (MacKenzie *et al.*, 2004) developed a technique that allows for the concentration of toxins present in water. This technique aims to provide an anticipated warning for the toxins in the water before the shellfish become toxic. The technique is known as Solid Phase Adsorption Toxin Tracking (SPATT) and consists of bags filled with porous resins

commonly used in chromatographic columns to separate compounds such as toxins placed in aquatic environment. However, these resins adsorb not only toxins, but also other compounds due the large size of their pores, which can lead to diminished selective efficiency for the HAB toxins and make the analysis more difficult.

Given the need of improving SPATT technology, this thesis aims to test the application of a new kind of nanomaterial, Covalent Organic Frameworks (COFs), as adsorbent to substitute the resins regularly used in SPATT devices. These nanomaterials have a large surface area for adsorption, uniform pore size, and they are highly stable and versatile (Chandra *et al.*, 2013). Due to their characteristics, COFs could help to improve the SPATT technique, thus improving the toxic HAB monitoring and diminishing their negative impact on the aquaculture industry.

1.2. Aims

The main goal of this thesis is to test the efficiency of the mesoporous material Covalent Organic Frameworks (COFs), to capture lipophilic biotoxins, namely Okadaic Acid (OA), which is the most important representative of Diarrheic Shellfish Poisoning (DSP) toxins. To do so, laboratory scale tests of adsorption/desorption of this toxin with the COF will be performed. The adsorption/desorption assays will give information about the adsorption kinetics and the adsorption isotherms of the chosen COFs for the target compounds. We will also study the possibility of reusing the COFs, as a major point of interest. COF selectivity for lipophilic toxins will be studied by mixing the lipophilic toxin with another highly representative hydrophilic toxin, Saxitoxin. Finally, the first SPATT devices with COFs will be prepared.

1.3. Document Organization

The present thesis is divided into 6 chapters, which are subdivided in several parts.

The first chapter is the introduction. In this chapter, a general background, motivation and the aims of this thesis are presented and the document organization can be found there, as well.

Chapter 2 is about the literature review, where the theoretical principals of this study can be found, and the previous knowledge about the subject in study.

In Chapter 3, Materials and Methods can be found. Here are described the experimental protocols used in this thesis.

In Chapter 4 are the results obtained of the performed experiments. The results are described, as well as the methods used to make the necessary calculations.

Chapter 5 is about the discussion of the results obtained. This chapter contains comparisons with other studies and with theoretical principals.

Finally, in Chapter 6 some conclusions and future recommendations are presented that will allow a posterior application of the studied methods.

2. LITERATURE REVIEW

2.1. Harmful Algal Bloom and Marine Toxin Production

Microalgae can be found in marine and freshwater environments and they are very important organisms since they are the base of food webs and they have an important role as CO_2 sinks and a carbon transporter to deep waters. Most of these algae are harmless, notwithstanding there are 2 % of marine algae species, which are known to produce toxins (Gilbert *et al.*, 2005; Scoging, 1998).

Harmful algal blooms (HABs) can be defined as microalgae overgrowths in water that somehow pose environmental or public health threats (Backer and Mcgillicuddy, 2006; NOAA, 2016). Most microalgae that overgrow are dinoflagellates or cyanobacteria, but other classes of algae, for example diatoms, have members that form HABs under the right conditions (Gilbert *et al.*, 2005). These out-of-control algae growths are a major environmental problem (US EPA, 2016b) that can lead to damages as hypoxia, anoxia and shading of submerged vegetation (Gilbert *et al.*, 2005). Toxin production may kill fish, mammals, and birds. They can also create dead zones in water (e.g. drinking water) rising treatment costs as a consequence. Some algal blooms are non-toxic, but they can cause damage to the aquatic ecosystem, discolor water or form huge and smelly piles of algae on beaches. Harmful algal blooms occur in freshwater environments as well (NOAA, 2016; US EPA, 2016a).

These phenomena occur naturally, but climate change and increasing nutrient pollution can increase their frequency of occurrence, intensity and the geographic distribution of HABs worldwide (Espiña *et al.*, 2015). Climate change has allowed these blooms to occur more often and in locations not previously affected. The increasing nutrient enrichment (mainly nitrogen and phosphorus) comes from anthropogenic activities (e.g. agriculture), which components flow into rivers, bays, and seas. There are other climate change effects that could influence the occurrence of HABs, such as warming water temperature, which is favorable for toxic blue-green algae to proliferate and allows them to float to the surface faster; salinity changes because with increasing global temperature droughts will be more common, which will make the freshwater saltier, allowing marine algae to invade freshwater ecosystems; higher carbon dioxide levels, enhancing algae

growth speed. The rise of the sea level and coast upwelling are also responsible for creating optimal conditions for algae proliferation, in the way that sea level rise stabilizes coastal water and coast upwelling brings nutrients from the bottom of the ocean to the surface (NOAA, 2016; US EPA, 2016a).

HABs with toxin production are not only a public health problem but also an economical problem. In the USA, coastal HABs have been estimated to result in economic impacts of at least 82 million dollars per year (NOAA, 2016). The costs resulting from HABs are related with direct expenses of public health and medical care, commercial and recreational fishing, tourism-related activities, water quality deterioration, and costs with sustained environmental monitoring (Gilbert *et al.*, 2005).

These phenomena rise the concern of public health concern because toxins can accumulate in organisms higher up in food webs, as for example shellfish. Toxins accumulate in the digestive gland of shellfish but these organisms are, in general, unaffected by them. Low concentration of algal cells in sea water (about 200 cells in each milliliter of water) may be enough to result in toxin accumulation in shellfish. On the other hand, shellfish can detoxify if it is moved to uncontaminated water, nevertheless depuration times may vary widely depending on the toxin nature, the bivalve species involved, and hydrographic concentrations (Scoging, 1998). Once other animals, including humans, consume affected organisms, they are exposed to toxins (Backer and Mcgillicuddy, 2006).

The toxins produced during a marine HAB are very extensive but the most common in our latitudes are: saxitoxins, responsible for Paralytic Shellfish Poisoning (PSP); domoic acid, responsible for Amnesic Shellfish Poisoning (ASP); okadaic acid and dinophysistoxins, responsible for Diarrhetic Shellfish Poisoning (DSP); and azaspiracids, responsible for Azaspiracid Shellfish Poisoning (AZP) (Gilbert *et al.*, 2005).

All of the above syndromes are characterized by a lack of organoleptic evidence of contamination in affected fish and shellfish (Scoging, 1998).

2.2. Diarrhetic shellfish poisoning

Diarrhetic Shellfish Poisoning (DSP) is a human foodborne intoxication caused by ingestion by humans of shellfish (e.g. mussels, scallops, oysters and clams) contaminated with DSP toxins,

including the okadaic acid (OA) group of toxins. Usually the DSP toxins, produced by dinoflagellates of the genera *Dinophysis* and *Prorocentrum*, are accumulated in the fatty tissue of shellfish due to their lipophilic nature. The symptoms, typical of gastroenteritis, are diarrhea, nausea, vomiting, abdominal pain, headache, chills, and fever starting between 30 min and 12 h after ingestion. Complete recovery occurs within 3 to 4 days. However, the affected individuals rarely need hospitalization and any treatment prescribed is only helpful to diminish the gastrointestinal effects. DSP most affected areas seem to be Europe and Japan, but North and South America, Australia, Indonesia, and New Zealand are affected as well (FAO, 2004; Lawley, 2013; Lloyd *et al.*, 2013; Scoging, 1998; Taylor *et al.*, 2013).

The first report of a gastrointestinal illness caused by dinoflagellates due to shellfish ingestion dates from 1961 in the Netherlands. Between 1976 and 1990, there were 10 000 DSP cases reported world-wide. However, due to the legislation applied since then, the incidences have decreased (Scoging, 1998). In Europe, major outbreaks of DPS have been reported. In 1990, mussels imported from Denmark caused 415 cases of illness in France. In 1984, 10 000 people in France were affected by DSP symptoms caused by domestically produced mussels. In the same year, another outbreak in Norway affected at least 300 people. In Spain in 1981, over 5 000 cases of DSP-related gastroenteritis were reported and OA toxins are periodically found at high levels in shellfish from Galician region. In UK, 1997, 49 people became ill after eating mussels in a restaurant in London. In Japan, at least 1 300 cases of DSP were reported between 1976 and 1981 (Lawley, 2013). In British Columbia, Canada, in 2011, 62 DSP illnesses occurred in July–August because of consumption of US Pacific Northwest Costal mussels (Lloyd *et al.*, 2013; Taylor *et al.*, 2013).

In Europe, the current legislation regarding DSP toxins in shellfish is Regulation (EC) No 853/2004 of the European Parliament and of the Council. It lays down specific hygiene rules for foodstuffs which claim that food business operators must ensure that live bivalve mollusks placed on the market for human consumption must not contain marine toxins in total quantities (measured in the whole body or any part edible separately) that exceed for okadaic acid, dinophysistoxins and pectenotoxins together, the limit of 160 μg of okadaic acid equivalents per kilogram (European Parliament & Council of European Union, 2004). In USA, Food and Drug Administration (FDA) regulatory guidance level for total OA equivalent is the same (Lloyd *et al.*, 2013).

2.3. Okadaic Acid Group of Toxins

Okadaic acid group of toxins (Figure 1) includes okadaic acid, dinophysistoxin-1 (DTX1), and dinophysistoxin-2 (DTX2). Together they constitute a heat stable and lipophilic polyether-type group of secondary metabolites usually produced by dinoflagellate algae. Dinophysistoxin-3 (DTX3) refers to a range of saturated and unsaturated fatty acids ester forms of OA, DTX1, or DTX2 found in phytoplankton and they are also products of shellfish metabolism (EFSA, 2008; FAO, 2004; Prego-Faraldo *et al.*, 2013; Taylor *et al.*, 2013).

The molecular structure of OA is characterized by a backbone of 38 carbons, 17 chiral centers, and 3 spiroketal moieties (McNabb, 2008). This chemical structure is represented in Figure 1, as well as the structures of dinophysistoxins. DTX1 and DTX2 are methylated analogues of OA, while DTX3 can be described as an acetylated analogue (Vieytes *et al.*, 1997).

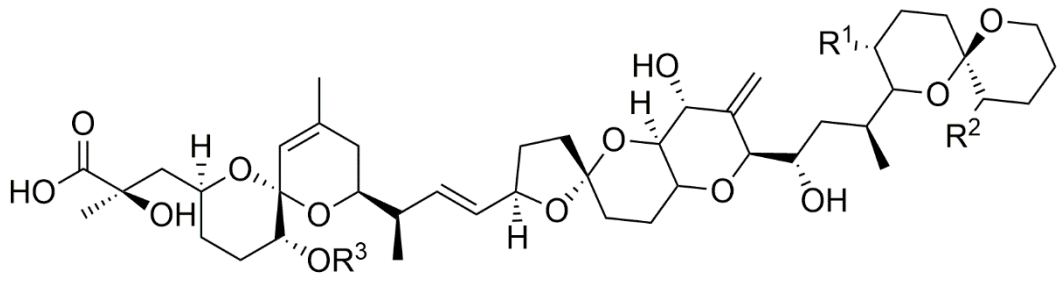

	R^1	R^2	R^3
OA	CH_3	H	H
DTX1	CH_3	CH_3	H
DTX2	H	CH_3	H
DTX3	CH_3	CH_3	Acyl

Figure 1 – Molecular structure of okadaic acid and dinophysistoxins.

OA is more heat stable than DTX2, degrading considerably at 120 °C, whereas DTX2 starts to degrade already at about 100 °C. In shellfish tissues these toxins are highly stable in the frozen state (–20 °C to –80 °C) for several months (EFSA, 2008).

OA and dinophysistoxins are known for being powerful inhibitors of serine/threonine protein phosphatase (PP) enzymes, especially PP-1 and PP-2A, the most common phosphatases in mammalian cells. However, OA is also an inhibitor of a range of others phosphatases, including PP-3 and PP-4 (McNabb, 2008). In PPs, OA binds to a region near the active site blocking their

activity. This leads to a hyperphosphorylation of the proteins that control sodium secretion by intestinal cells and cytoskeletal or junctional moieties that regulate solute permeability. Since permeability is favored, sodium is released, and a subsequent passive loss of fluids occurs, characterized by diarrheic symptoms. This process is summarized in Figure 2 (Garibo *et al.*, 2012).

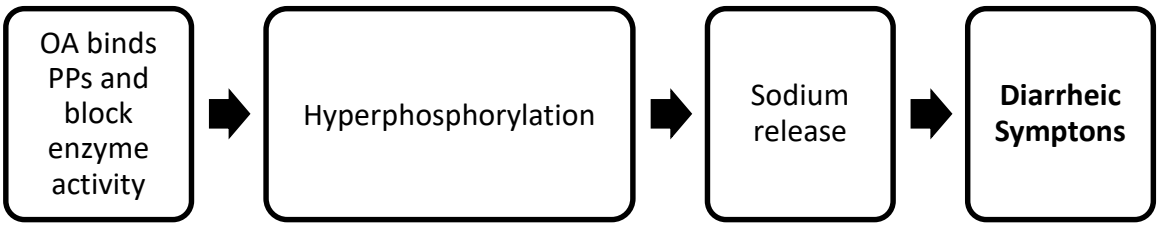

Figure 2 – OA inhibition process of PPs (Garibo *et al.*, 2012).

PP-1 and PP-2A are involved in the regulation of many cellular processes. PP-1 is tangled in several of cell functions, such as glycogen metabolism, synaptic plastic, and cell cycle control. On the other hand, PP-2A is implicated in the control of numerous cellular events, such as metabolism, apoptosis, cell cycle control, DNA replication, gene transcription, protein translation, and cell transformation. OA selectively inhibits PP-2A and, to a lower extent, PP-1. The IC_{50} values for PP-2A and PP-1 are in the ranges of $0.02 < \frac{IC_{50}}{\text{nmol L}^{-1}} < 0.2$ and $10 < \frac{IC_{50}}{\text{nmol L}^{-1}} < 100$, respectively (Tubaro *et al.*, 2008). IC_{50} can be defined as the value that indicates the concentration of a compound needed to inhibit by half a biological or biochemical function, e.g. inhibition of enzymes (Pharmacelsus, 2015).

The inhibitory activity of OA is related to its carboxylic acid group. Structural studies have shown that its removal or esterification is followed by a loss of activity (Espiña *et al.*, 2010). On the other hand, the hydroxyl groups across the structure also seem to play important roles in the interaction between the toxin and its target, with their modification leading to a significant decrease of PP inhibition (Tubaro *et al.*, 2008).

Besides being responsible for DSP, OA group of toxins can have other biological effects: they can influence the metabolism of glucose and lipids. The metabolism of glucose can be affected by OA through the inhibition of glycogen synthesis and an increase in the synthesis of glycogen. This particular effect is related to PP-1 inhibition, because this enzyme controls glycogen metabolism. OA can also influence the transport of glucose to the cells due to an insulin-like effect. However, in some cases, a decrease in the insulin-promoted glucose adsorption has also been detected. This

effect was observed in different cells, for example adipocytes of mice, rats, and humans (Tubaro *et al.*, 2008).

2.4. Monitoring HABs and Marine Toxin Production

Tracking down and predicting HABs can reduce drastically their impact on public health and the economy. To do so, HAB management strategies must be used. The most common of them is based on mitigation, where biotoxin content in shellfish is monitored by testing shellfish. These tests use methods of three kinds:

- Chemical. E.g.: Liquid Chromatography with Fluorescence Detection (LC-FD), Liquid Chromatography with Mass Spectrometry (LC-MS) and Capillary Electrophoresis (CE));
- Biological. E.g.: *in vivo* assays (mouse bioassay; rat bioassay); *in vitro* assays (cell culture assay);
- Biochemical. E.g.: phosphatase inhibition assays, ELISA, and immuno- or no immuno-based biosensors).

This strategy is currently applied in more than 50 countries (Anderson, 2009).

As seen above, there are several methods to detect biotoxins in shellfish and in Europe they are legislated by Commission Regulation (EC) No 2074/2005 and Commission Regulation (EU) No 15/2011 (EC, 2005, 2011). One of the most sensitive authorized method is LC-MS, which is currently the official method for detecting most part of biotoxins in shellfish. However, simpler methods permitted by law, such as biochemical assays (e.g. ELISA), are lower-priced. The mouse bioassay, which was the first method developed for biotoxin detection and still world-widely used, was eliminated in the European Union in January 31st of 2014 (Anderson, 2009; EC, 2011; Sassolas *et al.*, 2013).

Analyzing shellfish is the perfect tool to protect the health of the consumers but it does not prevent economic losses for the aquaculture industry. Additionally, this method has some drawbacks such as difficulty in procuring and preparing samples of shellfish, the different affinity for biotoxins of each species of shellfish. As shellfish become toxic over the regulated limits during a HAB, late after the initial phase, this method cannot be used as an early warning method. (MacKenzie, 2010; MacKenzie *et al.*, 2004; McCarthy *et al.*, 2014).

Phytoplankton monitoring is in general a reliable and cost-effective method of early warning for the development of HABs. However, it can cause unnecessary alerts, because the presence of toxin producer microalgae in the seawater does not necessary mean that toxins will be produced. Phycotoxins are a secondary product of microalgae metabolism, and it is not clear how and why they are produced; microalgae ecology, water eutrophication and climate were demonstrated as important factors in some cases but the complete causative scenario is unsolved yet. Thus, phytoplankton monitoring only provides information about the possibility of shellfish contamination. Besides, it is an intensive and time-consuming labor requiring highly trained staff, because discrimination between microalgal species involves detailed morphologic observations (MacKenzie, 2010; MacKenzie *et al.*, 2004; McCarthy *et al.*, 2014).

In USA, there are programs for HAB monitoring since the 1990's where volunteers collaborate with scientists. These type of initiatives can not only provide an early warning about these events but also contribute to educate population and increase community consciousness about this problem. These programs also raise sampling capabilities and reduce costs to the agencies (Jewett *et al.*, 2008; NCCOS, 2016).

The major goal of HABs management is to develop procedures designed for forecasting or accelerate the terminus of these toxic events. For this purpose, the above-mentioned methods are rather weak. Therefore, it is necessary to develop better tools for the detection and monitoring of HABs and resulting toxic events, which would also allow for a better understanding of the dynamics of a HAB (Zingone and Oksfeldt Enevoldsen, 2000). Emerging technologies exist, the aim of which is to simplify monitoring methods and to provide an early warning about HABs, avoiding public health problems and economic losses. For example, remote satellite sensing is also used to track HABs in the Gulf of Mexico. This is used to detect very dense and non-specific blooms, which have a chlorophyll signature to expose their presence. A method like this can be useful for tracking down blooms, however, it does not provide any information about the toxin presence (Anderson, 2009).

On a smaller scale, molecular probes for some toxic microalgae species have been developed that allow for a faster and easier detection and counting than traditional microscopy. The probes are usually antibodies or DNA segments, such as oligonucleotides, specific for algae species of interest (Anderson, 2009). The antibodies used to detect HAB species can be monoclonal or polyclonal and they provide a rapid and sensitive identification. However, the immunological techniques

depend on the identification of a phenotypic epitope that can be influenced by environmental factors. On the other hand, the creation of a monoclonal antibody can be seen as a drawback because it is time-consuming and costly (Hosoi-Tanabe and Sako, 2005).

The molecular biology technique FISH (Fluorescence *in situ* Hybridization) has been reported to be a simple and rapid technique to detect microalgae of *Dinophyceae* class. However, it requires specific equipment (epifluorescence microscope) (Hosoi-Tanabe and Sako, 2005).

Devices known as environmental sample processors (ESPs) are already used to sample surface water and measure its quality, and concentrate solid particles present in the sea (Espiña *et al.*, 2015). They use DNA analysis to identify microorganisms in these particles, evaluate the presence of algal toxins and measure their concentration and store the captured particles it takes for sample for posterior analysis. However, this device is limited by its volume (189.27 L) and in that it cannot chase after HABs that move with waves and marine currents. The 3rd generation of these devices, which will be able to travel for thousands of kilometers while performing a battery of scientific tests, is presently in the test phase and they will be able to follow HABs as they move. As a result, they will be capable of tracking and identifying toxic blooms before they arrive to the coast (Seltenrich, 2014). If the ESPs could be coupled with a device called *Imaging FlowCytobot*, the provided information would be more complete. *Imaging FlowCytobot* is a submarine automatic microscope, which delivers information about the algal cells *in situ* (Greenfield *et al.*, 2008; Seltenrich, 2014).

ESPs are a technology which needs to be improved. First, the sample needs to be the most homogeneous possible, so the test made *in situ* can be validated afterwards, and that is not always possible. The analyses that these kind of devices can make also need optimization (Doucette *et al.*, 2009; Greenfield *et al.*, 2008).

In China and Korea, tests of spraying of clay on the surface of water have been done to aggregate and sink algal cells to protect their fish industries from HABs. This method is effective in cleaning cells from the water (Seltenrich, 2014). Nevertheless, this mechanism for algae remove is not well-known. The engineering details and specification for size particle, concentration of clay, spreading method, and effective conditions are not recognized yet (Han and Kim, 2001).

The technologies reviewed above could represent solutions for the biotoxins problem. However, none of these methods are at the same time, simple, cost-effective and rapid. Thus, the need to

find a solution for an early detection and an effective capture of biotoxins is leading to new techniques development. Techniques which will be more precise and more sensitive and will prevent the negative impacts of those events.

2.5. Solid Phase Adsorption Toxin Tracking

In 2004, MacKenzie *et al.* proposed a new method to detect HABs based on the observation that, during HAB events there are significant amounts of polar and non-polar biotoxins dissolved in the seawater. This led to the development of a tracking device that is designed to adsorb the dissolved molecules, increasing biotoxin concentrations to levels that could be quantified, and providing a simple means for biotoxin monitoring (MacKenzie *et al.*, 2004).

The technique is known as Solid Phase Adsorption Toxin Tracking (SPATT) and it is similar to other passive sampling methods as seen in the point 3, in the way that concentrates biotoxins. (MacKenzie, 2010). SPATT devices consisted of bags made from polyester mesh, which contain a resin for the adsorption of algal toxins dissolved in sea water (Rundberget *et al.*, 2009). The bags are placed in a frame linked to a weighted line at formerly determined places and depths in the sea (Espiña *et al.*, 2015).

SPATTs have several advantages: it is simple and economical and the bags are easy to transport and store. The kind of sampling technique a SPATT uses can simulate toxin uptake by shellfish, making it an appropriate method for sites where shellfish do not appear naturally. The direct target molecules are toxins that do not suffer biotransformation. The used resin matrices are relatively clean, simplifying the toxin extraction and analysis. When allied to analysis methods, such as ELISA or LC-MS, this sampling method becomes very sensitive and can actually provide early information about the toxic blooms. Additionally, this method can offer information about toxin dynamics, such as the origin of new toxins, toxin environmental persistence, and variations on specific toxicity of the microalgae that produce toxins (MacKenzie, 2010; MacKenzie *et al.*, 2004).

The efficiency of SPATT as an early warning tool of toxic blooms depends on a number of factors, such as for example the amount of toxins released by cells and the toxin profiles of the toxic species in seawater. Toxin profile is dependent on sampling time and toxic algae distribution. It is also

necessary that toxins adsorbed by passive samplers reflect toxic algae vertical distribution in water body (Li *et al.*, 2011).

SPATT was shown to be useful to concentrate lipophilic toxins such as okadaic acid, pectenotoxins, azaspiracid, dinophysistoxins, and yessotoxins to a level capable of predicting toxic blooms, which affect shellfish with days or weeks in advance (Espiña *et al.*, 2015).

SPATT has also the potential to be a universal tool to trace other marine phycotoxins (e.g. ASP and PSP), freshwater toxins, and other waterborne pollutants such as polycyclic aromatic hydrocarbons (PAHs), polychlorinated biphenyls (PCBs), and other persistent organic pollutants (POPs) (Turrell *et al.*, 2007).

Since its development, the SPATT technique has been studied in attempt to find the best sorbent resin to be used for each type of toxin and for each aquatic environment. The passive adsorption in SPATT is more determined by the pore size of the resin than the surface area. The polarity of the analyte is another important factor in the adsorption (Li *et al.*, 2011).

The most common resin used thus far to track lipophilic toxins is DIAION1 HP-20, whose structure are represented in Figure 3. This resin is employed in HPLC for hydrophobic compounds, such as antibiotics and biomolecules, which makes it appropriate to trap lipophilic toxins. It consists of a styrene–divinylbenzene matrix, with a density of 1.01 g mL^{-1} and a surface area about 500 m^2 g^{-1} (Sigma-Aldrich Co. LLC., 2016). This resin also can accumulate more OA than the other resins and does not reach the equilibrium within 72 h probably because of its larger pore size (26 nm) (Espiña *et al.*, 2015; Sigma-Aldrich Co. LLC., 2016; Zendong *et al.*, 2014). The maximum OA that HP-20 can hold is 1 639 µg g^{-1} (Li *et al.*, 2011).

Zendong *et al.* compared several sorbent resins used for SPATT technique with different efficiencies and different accumulation speeds and concluded that there are some as *Strata*™-X polymeric Solid Phase Extraction (pore size: 16,2 nm; surface area: 767 m^2 g^{-1}) and *Oasis*® HLB (pore size: 18 nm; surface area: 799 m^2 g^{-1}), which are indicated for use in daily or *in situ* evaluation of toxin presence once they are fast accumulators, while HP-20 is indicated to be used for long exposure periods (>5 days) (Zendong *et al.*, 2014).

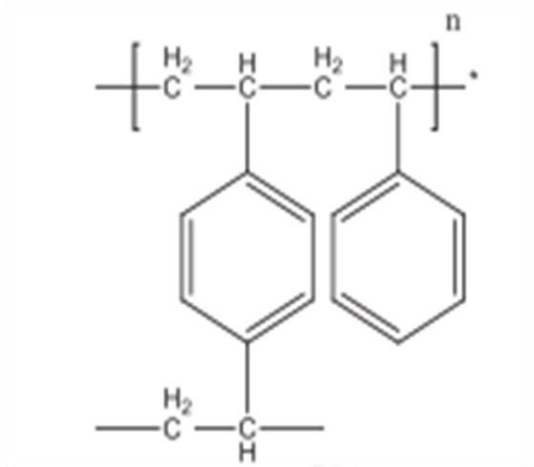

Figure 3 – The chemical structure of HP-20 resin (Zendong *et al.*, 2014).

As the SPATT technique has the potential to be a helpful tool in HABs early warning, the resins used to concentrate toxins are still a problem. They have a pore size which is much larger than the size of the toxin itself. When these resins are used they not only capture toxins, but they can also capture larger compounds or complexes. Consequently, there is a need for an adsorbent that can be more selective for toxins.

2.6. Covalent Organic Frameworks

Covalent Organic Frameworks (COFs) are a class of porous materials formed by the self-assembly of organic building blocks. These solids are lightweight and crystalline networks formed by robust covalent bonds between C, Si, B, N, and O. They also have high surface area, a very good stability in several solvents, including organic solvents and some even in water, tunable structures and pore size, low density, high pore homogeneity, versatile building units, high thermal stability, and permanent porosity. COFs have the potential to be used in several applications, such as adsorption, gas uptake and storage, and catalysis (Díaz and Corma, 2016; Ding and Wang, 2013; Feng *et al.*, 2012).

COFs can be two-dimensional (2D) or three-dimensional (3D), depending on the geometry of the building blocks. 2D COFs are composed of covalently bound 2D sheets, which are stacked further to form a layered eclipsed structure that grants periodically aligned and ordered columns. In 3D COFs, this framework is extended three-dimensionally by a building block containing a sp^3 carbon or silane atom (Feng *et al.*, 2012).

Since their discovery in 2005 by Yaghi and co-workers (Côté *et al.*, 2005), 2D COFs synthesized by B–O bonds have been widely studied. They usually feature high crystallinity but have low chemical stability and often decompose when exposed to water vapor. This limits their use in gas storage, catalysis, and adsorption applications. This problem was partially overcome by improving framework robustness using imine linkages in 2D COFs. These and further linkages are shown in Figure 3 (Ding and Wang, 2013). To improve COF stability in water, Banerjee and co-works (Chandra *et al.*, 2013) used the building block triformylphloroglucionol (Figure 4, bottom) and created the TpBD-Me_2 COF. The high stability is due to the 3-fold symmetric building block, which in the synthesis undergoes first a reversible imine-bond formation, and then an irreversible tautomerization, which locks the TpBD-Me_2 COF structure. This is the reason why this COF has an extremely high water-stability, much more than other imine linkages.

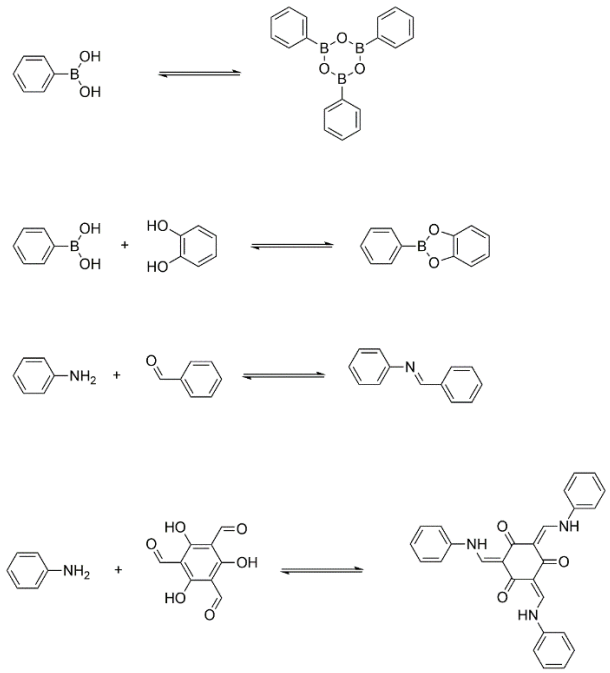

Figure 4 – Different covalent bonds used to construct COFs.

COFs have attractive characteristics for them to be applied in biotoxin capture, such as their high surface area, stability in water and in most of organic solvents, and even in alkaline or acid media (Chandra *et al.*, 2013). Comparing with the most used resin in the SPATT technique, HP-20, COFs show similar or higher surface areas but much smaller pore sizes, so they may offer a more selective capture when compared with HP-20. The smaller pore size is suitable with the molecular size of OA, so by using COFs, the selectivity for OA capture is expected to be improved. The COF

stability under different environmental conditions, as for example changes of water pH, may make it the perfect replacement for the commonly used resins.

The COF TpBD-Me_2 (Chandra *et al.*, 2013), the structure of which is shown in Figure 5, will be studied in this thesis to adsorb lipophilic biotoxins, such as OA and its derivatives. This COF was chosen for this work because, as said above, it is very stable in water and its pores are lipophilic, with methyl groups in the cavity (Chandra *et al.*, 2013). The lipophilic nature of the pores will not only favor the adsorption of lipophilic toxins, but retain them as well. The SPATT technique will be applied by replacing the conventional resins with the COF. TpBD-Me_2 COF has a pore size of 2.3 nm and a BET surface area of 468 $m^2\ g^{-1}$ (Chandra *et al.*, 2013). As the pore size of this COF is closer to the size of OA molecule as compared to that of HP-20, a more efficient and selective binding is targeted. In annex I are showed the porosity data and SAXS data of the TpBD-Me_2 COF sample example.

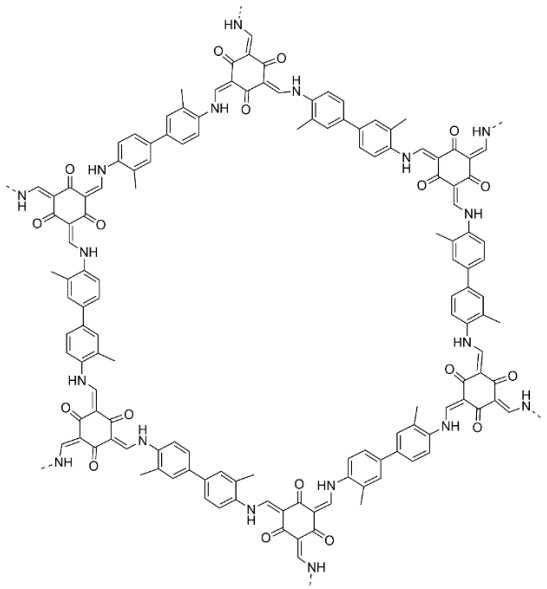

Figure 5 – The structure of one pore of TpBD-Me_2 COF (Chandra *et al.*, 2013).

2.7. Adsorption

Adsorption is a separation process based on mass transfer velocity, in the presence or not of a chemical reaction, and implies an intimate contact between two phases (solid–liquid or solid–gas). The driving force is the diffusivity of a liquid in the pores of a solid surface. Applying adsorption could be with the purpose of purification (e.g., treatment of liquid or gaseous effluents, recovery of

biological compound from fermentation, such as antibiotics, vitamins or flavoring compounds) or to separate compounds of a mixture (e.g., chromatography) (FCTUC - Departamento de Engenharia Química, 2007; Seader and Henley, 2006; Vermeulen *et al.*, 1984). Adsorption is also the most used technique worldwide to remove pollutants from contaminated media (Qiu *et al.*, 2009).

As adsorption is a phenomenon of surface, when molecules of liquid or gaseous phase (adsorbate) diffuse, they bind or interact with the solid surface (adsorbent) through weak intermolecular forces, such as van der Waals' forces, forming a monolayer at not extreme temperatures. At temperatures above 200 °C, the activation energy is high enough to make or break chemical bonds. When this mechanism prevails, the adsorption is called chemisorption or activated adsorption (FCTUC - Departamento de Engenharia Química, 2007; Vermeulen *et al.*, 1984).

The adsorption capacity depends on the type and the size of the pores. It also depends on the pore distribution and the nature of adsorbent surface. This is the reason why good adsorbents need to have a large surface area in association with a porous structure (FCTUC - Departamento de Engenharia Química, 2007).

The pores are classified in function of their diameter: pores with more than 50 nm of diameter are macropores, pores with diameters between 2 nm and 50 nm are mesoporous, and pores with less than 2 nm of diameter are micropores (FCTUC - Departamento de Engenharia Química, 2007).

The adsorbents commonly used are activated alumina, silica gel (of small pore or large pore), activated carbon (of small pore or large pore), molecular sieves, such as zeolites, and polymeric adsorbents. Their characteristics are summarized in Table 1.

Adsorption in liquid phase is more difficult to measure experimentally or describe than adsorption in gaseous phase. When the fluid is a liquid, the procedures to determine the adsorption of a pure liquid are not simple. Thus, experiments are made with liquid mixtures and dilute solutions. When the liquid mixture is in contact with the adsorbent, the pores, if they have diameter larger than the molecules in the liquid, fill with liquid. In equilibrium, the composition of the liquid mixture in the pores differs from the composition of the bulk that surrounds the pores (Seader and Henley, 2006).

Table 1 – Principal Proprieties of Commercial Adsorbents (Seader and Henley, 2006)

Adsorbent	Pore diameter, d_p/ nm	Particle porosity, ε	Surface Area, S/ (m^2 g^{-1})
Activated alumina	[1;7.5]	0.50	320
Silica gel:			
Small pore	[2.2;2.6]	0.47	[750;850]
Large pore	[10;15]	0.71	[300;350]
Activated Carbon:			
Small pore	[1;2.5]	[0.4;0.6]	[400;1200]
Large pore	>3	–	[200;600]
Zeolites	[0.3;1]	[0.2;0.5]	[600;700]
Polymeric Adsorbents	[2.5;4]	[0.4;0.55]	[80;70]

In adsorption, adsorbate partition between the liquid phase and the adsorbent implicates a dynamic phase equilibrium based on thermodynamics principles. This equilibrium can be described simply by expressing the quantity of solute adsorbed per quantity of adsorbent, q, as function of the equilibrium concentration of the solute in solution, C_e. This is called the adsorption isotherm. The graphic representation of an adsorption isotherm can take different forms. A linear isotherm is an attribute of absorbents with very homogeneous surfaces and it occurs normally for low solution concentrations. The most frequent isotherm is the favorable one; the unfavorable isotherm is typical of heterogeneous surfaces (FCTUC - Departamento de Engenharia Química, 2007).The graphic representations of these isotherms can be seen in Figure 6.

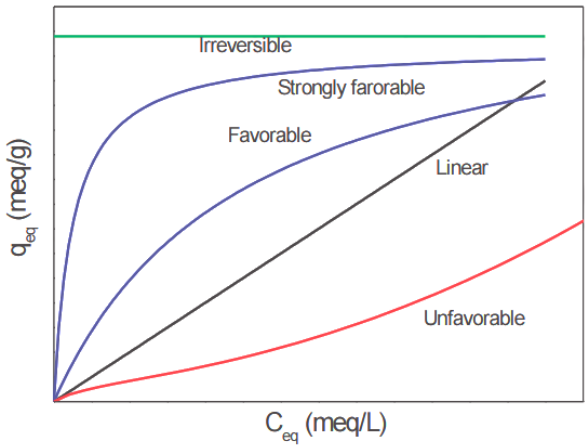

Figure 6 – Graphical representation of the various types of isotherms (Barros *et al.*, 2013).

In liquid adsorption, with a binary mixture and only in diluted solution, the amount of adsorption of the solvent, if there is any, may be constant and all the changes in the adsorbed quantity are just due to the solute. In these cases, the isotherms take the form of the ones obtained with pure gases. Thus, this type of data can be fitted using the Freundlich equation (equation 1) or the Langmuir equation (equation 2), where K represents a constant that depends on the temperature and the energy of the adsorption, and q_m represents the maximum of the adsorbed quantity (FCTUC - Departamento de Engenharia Química, 2007; Seader and Henley, 2006).

$$q = KC_e^{1/n} \quad \text{(equation 1)}$$

$$q = \frac{Kq_m C_e}{1+KC_e} \quad \text{(equation 2)}$$

The Langmuir model makes some assumptions, e.g., the surfaces of adsorbents are homogeneous, every active site has an equal affinity for the solute and there are not interactions between adsorbed molecules. It also assumes that a monolayer of adsorbate molecules is formed and that the adsorption is reversible (FCTUC - Departamento de Engenharia Química, 2007).

The Freundlich model has a parameter, $1/n$, that defines the degree of heterogeneity of the surface. When $n > 1$, the isotherm is favorable; when $n < 1$, the isotherm is unfavorable. It also assumes that the quantity absorbed tends to be infinite. The Freundlich model fits very well experimental data only in a moderate solute concentration range (FCTUC - Departamento de Engenharia Química, 2007).

For adsorption to occur, there are four steps needed:

1. External mass transfer of the solute from the bulk fluid though a thin film to the outer solid surface of adsorbent;
2. Internal mass transfer of the solute by pore diffusion from the external surface of the adsorbent to the internal pores of the adsorbents;
3. Surface diffusion along the porous surface;
4. Adsorption of the solute onto the porous surface.

These four steps are represented in Figure 7.

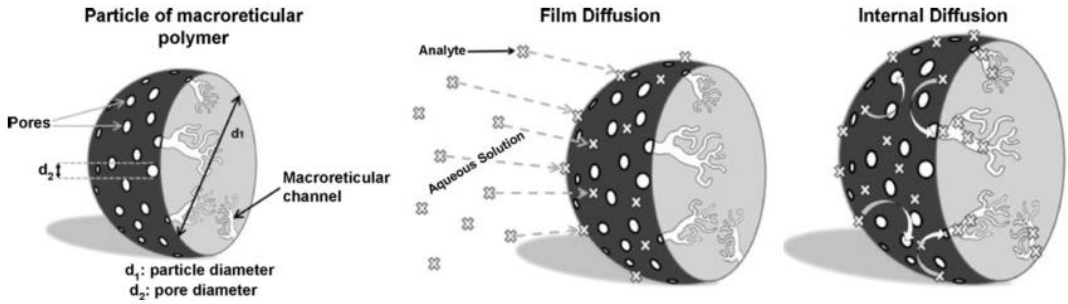

Figure 7 – How an analyte diffuses in a common adsorbent (Fux *et al.*, 2008).

To regenerate the adsorbent the four steps need to occur in reverse order to desorb the molecules. Both adsorption and desorption are convoyed by heat transfer. Adsorption is exothermic and desorption is endothermic (Seader and Henley, 2006).

The internal mass transfer of the solute into the pores can be evaluated by the coefficient of effective diffusivity, D_{ef} (equation 3) (FCTUC - Departamento de Engenharia Química, 2007).

$$D_{ef} = D_m \frac{\varepsilon_p}{\tau_p} \qquad \text{(equation 3)}$$

In this equation, D_m is the coefficient of molecular diffusivity, ε_p the porosity, and τ_p the tortuosity factor. The molecular diffusivity at infinite dilution can be calculated by the Wilke–Chang correlation (equation 4) (FCTUC - Departamento de Engenharia Química, 2007).

$$D_m = 7.4\times10^{-8} \frac{(2.6M)^{1/2}}{\mu V_m^{0.6}} T \qquad \text{(equation 4)}$$

Where M is the molecular weight of the solvent (g mol^{-1}), T is temperature (K), V_m the molar volume (cm^3 mol^{-1}), and μ the viscosity of the solution (cp[1]).

When an adsorption process is applied, kinetic aspects must be taken in consideration to know more details about the performance and mechanisms. Kinetics give information about how much solute is adsorbed in a time interval. It is essential to know the kinetics of a given adsorbent for

[1] 1 cp = 10^{-3} Pa s

pilot application. Their analysis allows to establish the solute uptake rate, which determines the residence time needed for completion of adsorption reaction (Qiu *et al.*, 2009).

There are many mathematic models that can describe adsorption kinetics. The one that will be used in this thesis is Pseudo-First Order Kinetics Model of Langergreen. This model is the most used to evaluate adsorption kinetics in liquid–solid systems and it is described by equation (equation 5).

$$\frac{d_{q_t}}{d_t} = k_1\left(q_e - q_t\right) \Leftrightarrow q_t = q_e\left(1+e^{-\frac{k_1}{2.303}t}\right) \qquad \text{(equation 5)}$$

Where q_t is the quantity of solute adsorbed in each instant, q_e is the quantity of solute adsorbed in equilibrium, k_1 is the first order kinetic constant (min^{-1}), and t represents time (min). This model also assumes that the velocity of the solute with time is directly proportional to the difference in saturation concentration and the number of active sites of the adsorbent (Carvalho *et al.*, 2010).

3. MATERIALS AND METHODS

3.1. Covalent Organic Frameworks Synthesis

Covalent Organic Frameworks (COFs) were prepared at INL in the Nanomaterials Synthesis Unit following the method proposed by Chandra and co-workers in 2013 (Chandra *et al.*, 2013.)

3.2. Quantification of Okadaic Acid (OA)

3.2.1. Preparation of Protein Phosphatase-1 (PP-1) enzymatic reaction buffer:

The buffer used for the PP-1 enzymatic activity was prepared by dissolving Tris-HCl, with concentration, *c*, c = 20 mmol L^{-1}, $MgCl_2$ (c = 5 mmol L^{-1}), $MnCl_2$ (c = 5 mmol L^{-1}) 2-mercaptoethanol (c = 0.1 % (v/v)), and Bovine Serum Albumin (BSA) (c = 1 mg mL^{-1}) in ultrapure water. The pH was adjusted to 8.00. All reagents were from *Sigma-Aldrich®.*

3.2.2. Preparation of DiFMUP Stock Solution:

DiFMUP (6,8-Difluoro-4-Methylumbelliferyl Phosphate) (*ThermoFisher Scientific®*) is a fluorinated 4-methylumbelliferyl phosphate (MUP) derivative that has a lower pKa than that of MUP, making DiFMUP an excellent substrate for continuously assaying acid phosphatases at low pH. The reaction product of DiFMUP has excitation/emission maxima of ~358/450 nm. DiFMUP stock solution (c = 40 mmol L^{-1}) was prepared by dissolving 5 mg of DiFMUP powder in a 50 mmol L^{-1} Tris-HCl solution.

3.2.3. Preparations of OA Stock Solution:

OA stock solution (c = 1 mmol L^{-1} or c = 2 mmol L^{-1}) was prepared by dissolving 100 µg of OA isolated from *Prorocentrum* sp. (*Merck Chemicals®*, UK) in 100 % ethanol.

3.2.4. Preparation of Protein Phosphase-1 (PP-1) Stock Solution:

Protein phosphatase1 (PP-1) is a heterodimeric enzyme with serine/threonine phosphatase activity. It comprises a catalytic subunit and a targeting subunit or a specific protein inhibitor. Protein Phosphatase-1 Catalytic Subunit, expressed in *E. coli*, was purchased in lyophilized powder

from *Sigma-Aldrich®*. PP-1 stock solution (c = 65.00 mkat L^{-1}) was prepared by dissolving 28.5 µg of protein in powder (enzymatic activity of 1.652 kat g^{-1}) in a solution of glycerol (c = 200 mL L^{-1}).

3.2.5. OA Quantification by Determination of Protein Phosphatase-1 Enzymatic Activity Inhibition:

Serial dilutions of OA were prepared in synthetic sea water for the calibration curve (Annex II). Intermediate solutions of PP-1 and DiFMUP, with concentrations of 41.67 µkat L^{-1} and 4 mmol L^{-1} respectively, were prepared in reaction buffer.

In each wells of a microplate 165 µL of reaction buffer, 10 µL of PP-1 intermediate solution, and at last 20 µL of OA serial dilutions or unknown sample were added. The microplate was incubated during 30 minutes at 37 °C in constant shaking (400 min^{-1}). After that time 5 µL of DiFMUP intermediate solution were added to each microplate well and the reaction occurred at 37 °C, constant orbital shaking (400 min^{-1}) during 2 h.

Then, fluorescence was read at 470 nm wavelength in a microplate reader in *Synergy H1™ Hybrid Multi-Mode Microplate Reader* by *BioTek® Instruments, Inc.* (DiFMUP excitation wavelength = 315 nm; DiFMUP emission wavelength = 470 nm; Optics position = Top)

3.3. Adsorption Kinetics Assay

A 1 mg mL^{-1} COF solution was prepared and 50 or 100 µL were used in each microtube. The needed volume of OA stock solution (c = 1 mmol L^{-1} or c = 2 mmol L^{-1}) was added in each microtube to the final concentration; 10 µmol L^{-1}, 15 µmol L^{-1}, 25 µmol L^{-1}, 50 µmol L^{-1}, and 100 µmol L^{-1}. The microtubes were incubated at 19 °C in constant shaking (1 400 min^{-1}). Microtubes were taken after 0 min, 1 h, 4 h and 8 h of incubation. Then, microtubes were centrifuged at 15 000 min^{-1} for 15 min and the supernatant was recovered. OA concentration in the supernatant was quantified by using the procedure described in section 3.1.5..

3.4. Desorption Assay

Pellets of COFs from the adsorption assays were re-suspended in 200 µL of 70 % ethanol or acetonitrile.

Those samples were incubated overnight, at 4 °C, in constant shaking (1 400 min^{-1}). Each sample was centrifuged at 15 000 min^{-1} for 15 min and the supernatant was recovered. OA concentration in the supernatant was quantified by using the procedure described in section 3.1.5..

3.5. Recycling tests

For recycling tests, pellets from desorption assays were washed by re-suspendending in 200 µL of ultrapure water, and then centrifuged at 35 000 xg, during 15 min at 21 °C. Supernatants were discarded and pellets were further used for new adsorption assays. Adsorption with OA concentration of 10 µmol L^{-1} was repeated, for a single time point at 4 h incubation. Afterwards, desorption assay was repeated with 70 % ethanol or acetonitrile.

This procedure was repeated 2 times for each pellet reused.

3.6. Tests with mixtures of toxins

The tests with mixtures of toxins followed the same procedure of the adsorption assays described in section 3.2., but adding equimolar concentrations of Saxitoxin and OA (c=10 µmol L^{-1}). Saxitoxin (STX), a neurotoxin isolated from marine dinoflagellates *Alexandrium tamarense,* was purchased from *Biorbyt®*, UK. OA concentration in the supernatant was quantified by using the procedure described in section 3.1.5.. Due to time constraints STX specific quantification was not included in this study.

3.7. SPATT laboratory prototypes devices

Two types of SPATT laboratory prototypes devices were fabricated; the first one by filtering 50 mg of COFs suspended in 100 % ethanol through a nylon mesh of 1µm pore size under vacuum. COFs were encapsulated in the nylon mesh by sealing against another piece of the nylon mesh were glued with a compatible polymeric resin from *Huntsman*, USA. The second prototype was fabricated using dialysis bags of 12.5 KDa of pore size. For evaluation of the SPATT stability in seawater both of them were placed in a vessel with synthetic sea water and incubated at room temperature in agitation for a week. After one week, the SPATTs prototypes were washed with ultrapure water and further transferred to a vessel containing 70 % ethanol or acetonitrile and incubated overnight in agitation at 4 ºC in order to mimic the procedure for toxin desorption. After

that, the prototype SPATTs were left drying at laboratory temperature and pressure for 2-3 days. The whole procedure was repeated at least two consecutive times.

3.8. Statistical Analysis

For adsorption kinetics, the squared error method, based in the squared difference between the data obtained and the value expected theoretically (using the equation of the kinetic models) are calculated, was used. The correlation coefficients were obtained by equation 6.

$$R^2 = 1 - \frac{\sum (q_{ex} - q_t)^2}{\sum (t - \bar{t})^2} \qquad \text{(equation 6)}$$

The equation relates the sum of square errors of the experimentally obtained absorbed quantity, q_{ex}, and the absorbed quantity calculated by the model, q_t, and the sum of the square error of time (subtraction between time, t, and the average of time, $\bar{t}$, squared).

Standard Deviation was calculated to know the experimental associated error.

The Freundlich isotherm was obtained by a linear regression.

4. RESULTS

4.1. Adsorption Kinetics

Initial concentrations of okadaic acid of 10 µmol L^{-1}, 15 µmol L^{-1}, 25 µmol L^{-1}, 50 µmol L^{-1}; 100 µmol L^{-1} were used at different incubation time points based adsorption assays to establish the adsorption kinetics of OA in COF as described in Materials and Methods section. The obtained kinetic curves are represented in Figure 8, Figure 9, Figure 10, Figure 11, and Figure 12, respectively. When the absorbed quantities obtained experimentally were plotted in function of time, the curve resembled the shape of a first order kinetics. Thus, a model of pseudo-first order kinetics (model of Langergreen) was used to fit the experimental data, because this model is described by the equation 5. The experimental data were fitted by *Solver* supplement of *Microsoft Excel®* (non-linear fitting). The values of q_e, k_1 and the correlation coefficient, R^2, of each kinetic curve are summarized in Table 2.

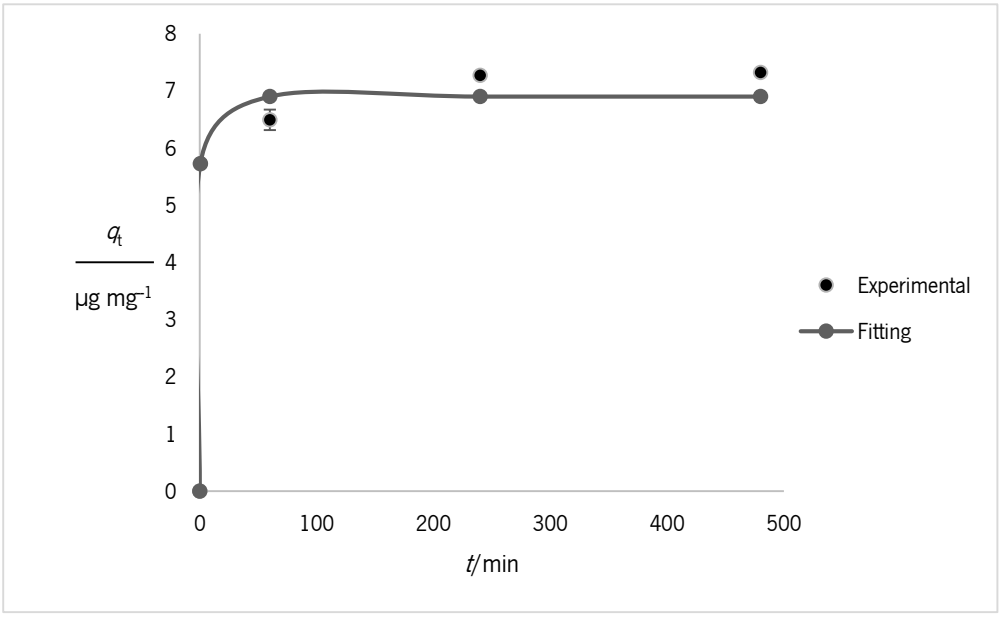

Figure 8 – Adsorption kinetics for initial concentration of OA of 10 µmol L^{-1}.

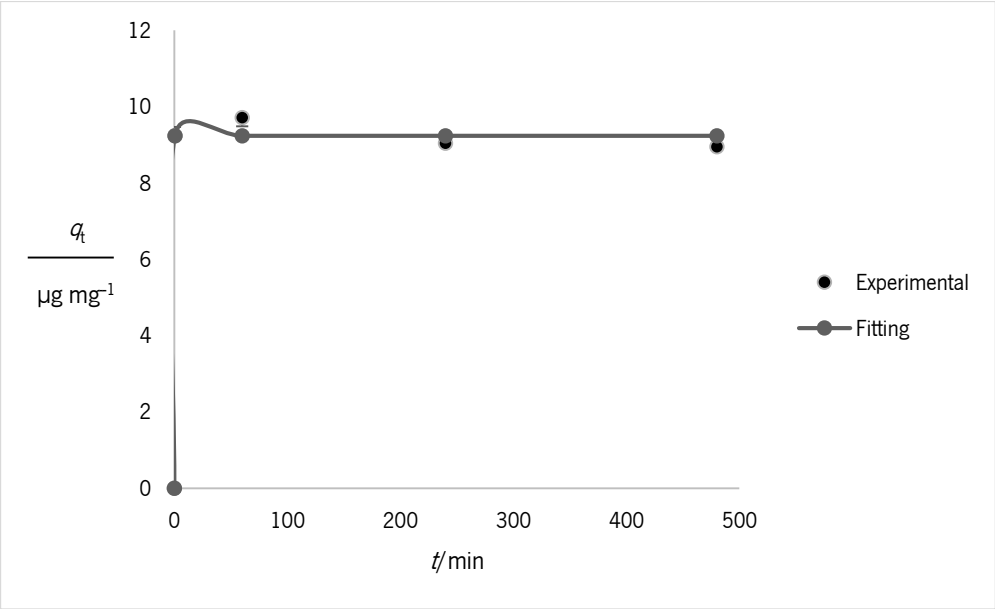

Figure 9 – Adsorption kinetics for initial concentration of OA of 15 μmol L^{-1}.

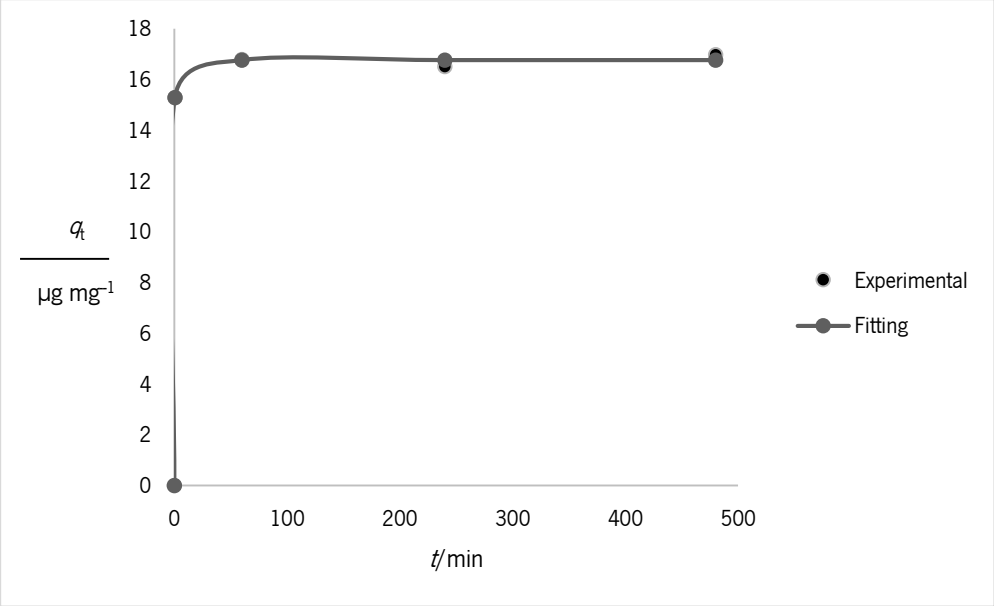

Figure 10 – Adsorption kinetics for initial concentration of OA of 25 μmol L^{-1}.

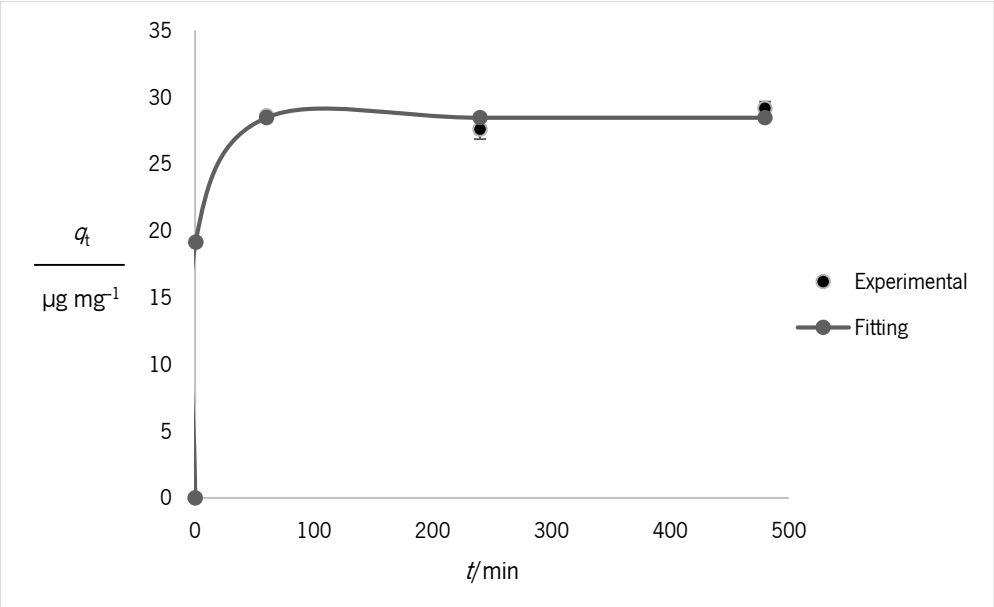

Figure 11 – Adsorption kinetics for initial concentration of OA of 50 µmol L^{-1}.

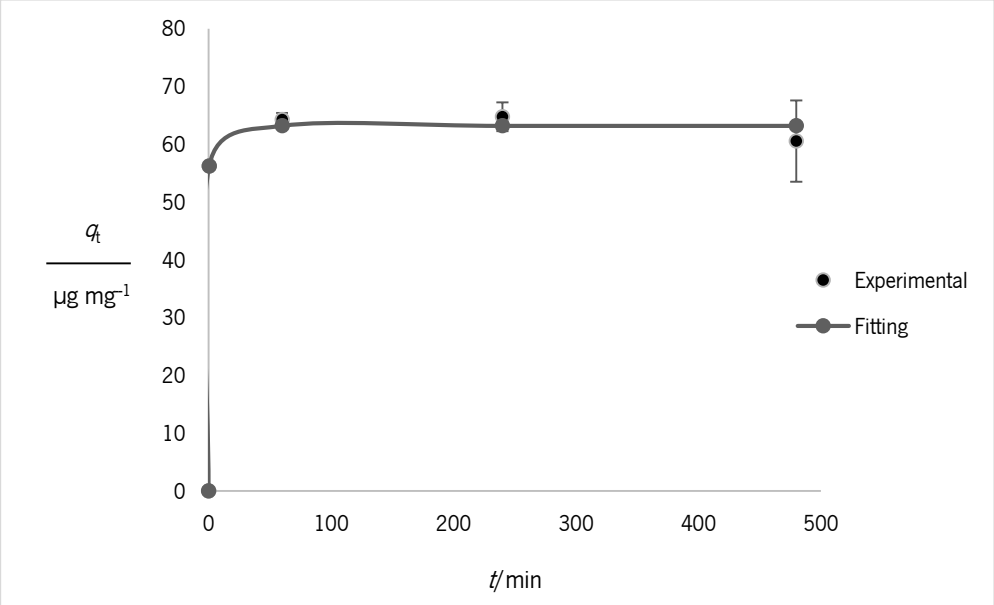

Figure 12 – Adsorption kinetics for initial concentration of OA of 100 µmol L^{-1}.

As observed in the adsorption kinetic graphics, the equilibrium is reached in short times (about 60 minutes), independently of the initial concentration of OA. As expected, a direct positive relationship between the initial OA concentration and the quantity absorbed in equilibrium, q_e was observed. Thus q_e increased as the initial concentration of OA did.

The correlation coefficients were obtained by equation 6. As shown in Table 1, the curves have high R^2 (about 0.99). Thus, the adsorption kinetic curves fit the model applied.

Table 2 – Kinetic Parametres

[OA] / (μmol L^{-1})	q_e/ (μg mg^{-1})	k_1/min^{-1}	R^2
10	6.900	7.817	0.983
15	9.238	59.195	0.996
25	16.759	10.699	0.999
50	28.458	4.927	0.998
100	63.214	9.708	0.997

4.2. OA Adsorption Capacity by COF

We compared the adsorption results for the different OA initial concentrations tested at an incubation time point when the equilibrium was reached (4 h) The percentage of OA captured, *PC*, was calculated dividing the amount of OA quantified by the amount of OA added for each adsorption assay. The error was calculated using the command DESVPAD.P of *Microsoft Excel®*. The results are represented in Figure 13. In this case, the higher percentage of capture was 90.925 % ± 4.372 % and it was achieved with an initial concentration of OA of 10 μmol L^{-1}. In general, at higher initial concentrations, the percentage of capture is around 75 %. This fact indicates that the highest OA initial concentration tested is still far from the saturation concentration for the COF. Unfortunately, it was impossible to increase the highest tested concentration experimentally due to the cost of the OA standard.

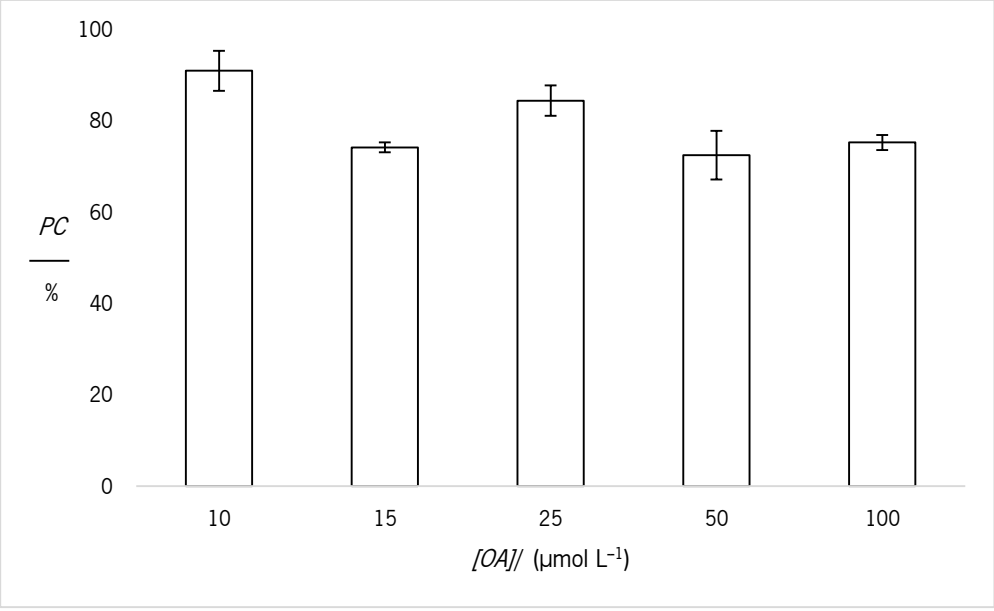

Figure 13 – Percentage of OA Captured, *PC*, in function of initial concentration of okadaic acid, *[OA]*.

4.3. Desorption Assays

The percentage of OA recovered from the COFs on the desorption assays, *PR*, are represented in Figures 14, and 15. The figures corresponding to the desorption of the OA from the pellets of the adsorption experiments with the lowest and highest OA initial concentrations (10 μmol L^{-1}, and 100 μmol L^{-1}, respectively). Desorption was performed separately with two different solvents: 70 % ethanol and pure acetonitrile. The error was calculated by using the command DESVPAD.P of *Microsoft Excel®*.

As it can be observed in Figure 14 all the initially added toxin was recovered with 70 % ethanol as well as with acetonitrile for the pellets with the concentration of 10 μmol L^{-1}. 70 % Ethanol showed slightly better results, including an overestimation due to the experimental variability. Figure 15 shows that desorption efficiency drops to around 60 % when the initial concentration of OA was 100 μmol L^{-1}. Thus, desorption of the adsorbed OA in COF is not complete when using the same conditions as for the 10 μmol L^{-1} initial concentration. In any case, acetonitrile showed a slightly worse performance to recover OA.

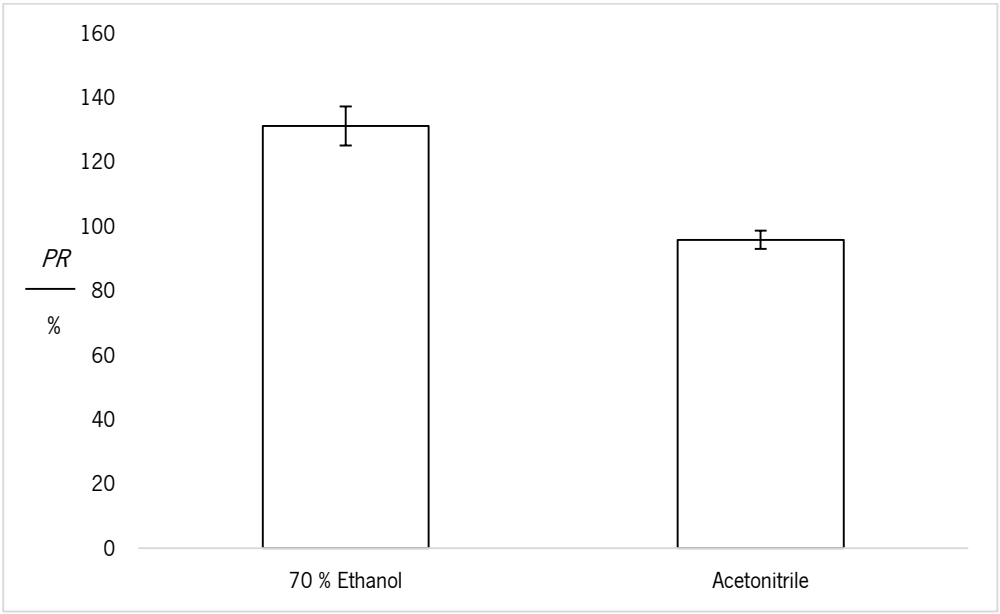

Figure 14 – Percentage of OA recovered, *PR*, after desorption of pellets of adsorption assay of 10 μmol L^{-1} with 70 % ethanol and pure acetonitrile.

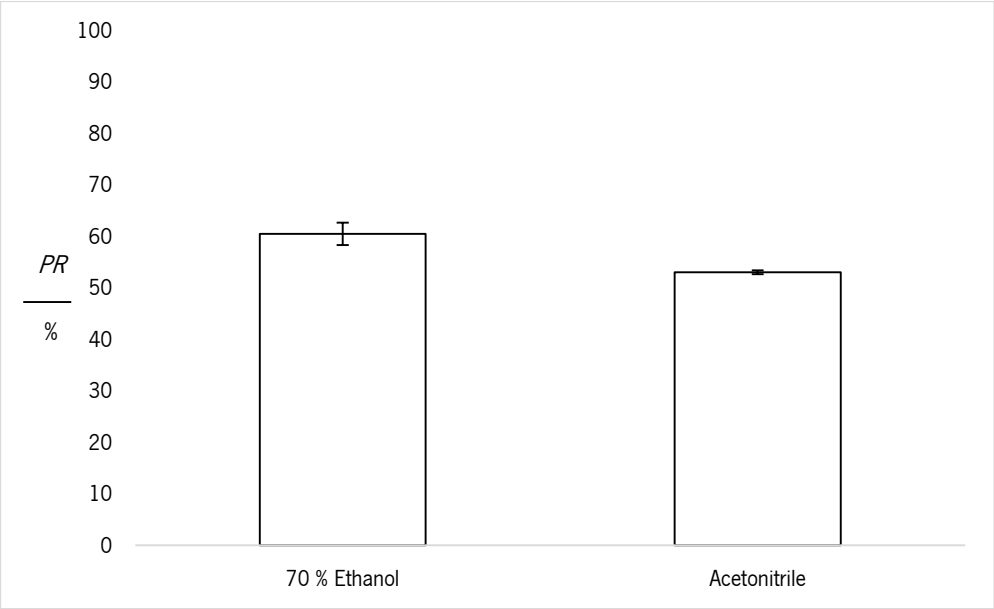

Figure 15 – Percentage of OA recovered, *PR*, after desorption of pellets of adsorption assay of 100 µmol L^{-1} with 70 % ethanol and pure acetonitrile.

4.4. Coefficient of Molecular Diffusivity and Coefficient of Effective Diffusivity

In Figures 16, 17, 18, 19 and 20 the coefficients of molecular diffusivity, D_m, and the coefficients of effective diffusivity, D_{ef}, are shown as a function of the time. Those parameters were calculated for each adsorption assay using equation 3 and equation 4, respectively. Both coefficients have similar values as it can be noticed due to the fact of being completely overlapped in the graphs. The values obtained corroborate the adsorption kinetics results, since with the increase of the initial concentration of OA, the velocity of diffusion is higher. The higher velocity of diffusion was since they show a quick velocity of diffusion, always below 5×10^{-4} $cm^2 s^{-1}$, as shown in Figure 20, which is 500 000 000 μm^2 s^{-1}.

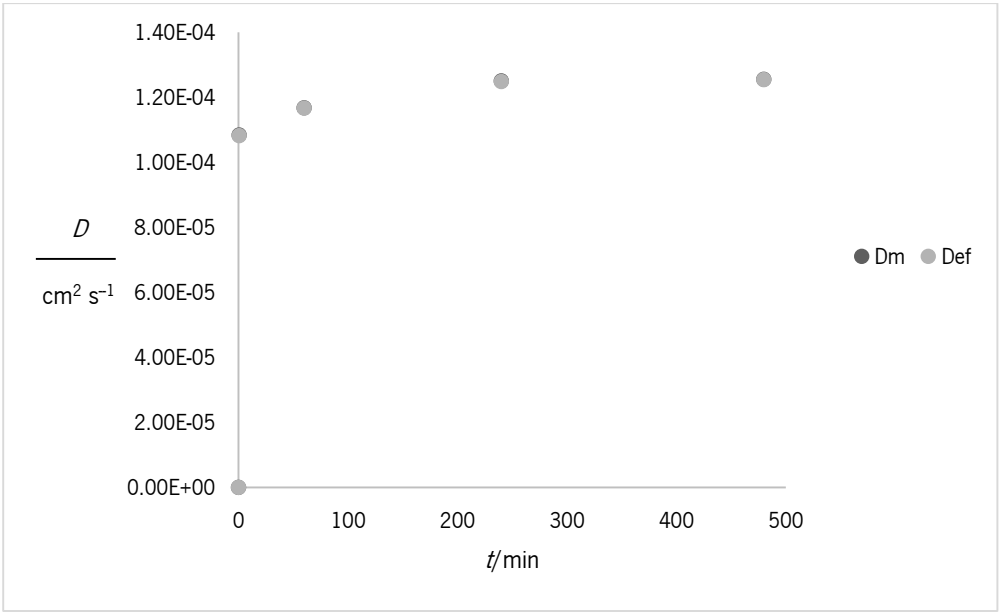

Figure 16 – Coefficients of molecular diffusivity, D_m, and coefficients of effective diffusivity, D_{ef}, expressed as a function of time for an initial concentration of OA of 10 μmol L^{-1}.

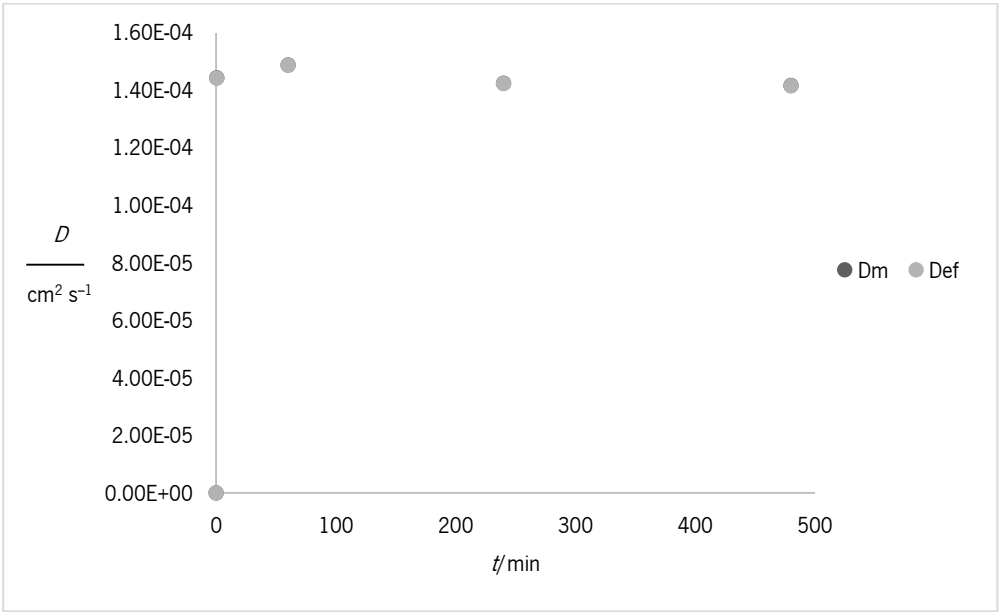

Figure 17 – Coefficients of molecular diffusivity, D_m, and coefficients of effective diffusivity, D_{ef}, expressed as a function of time for an initial concentration of OA of 15 μmol L^{-1}.

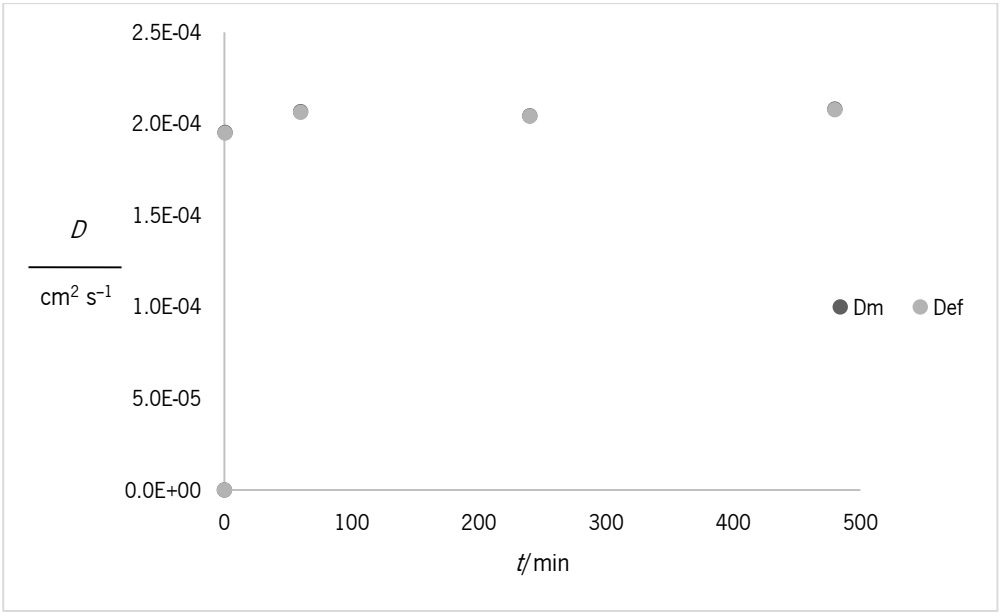

Figure 18 – Coefficients of molecular diffusivity, D_m, and coefficients of effective diffusivity, D_{ef}, expressed as a function of time for an initial concentration of OA of 25 μmol L^{-1}.

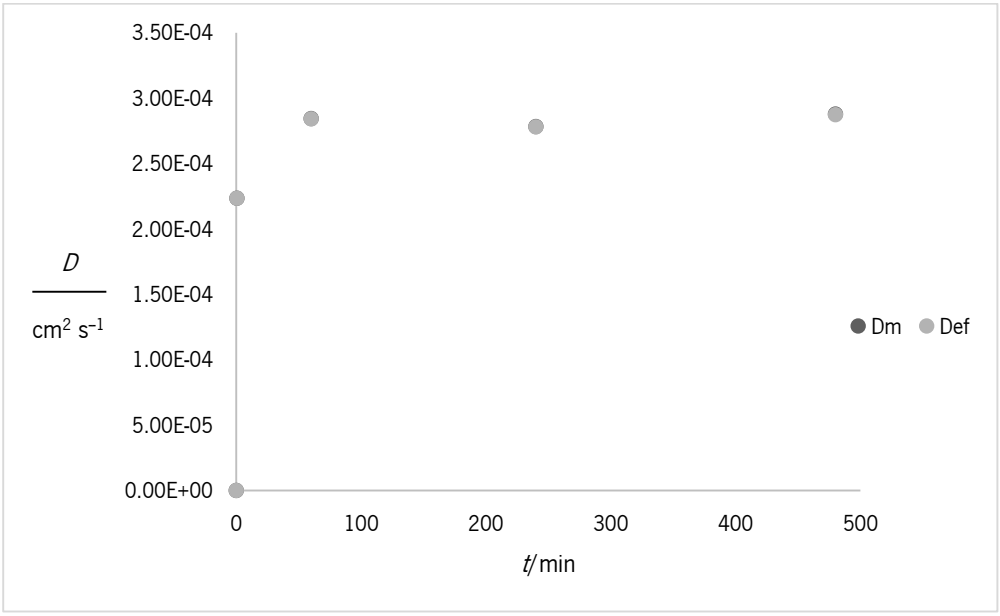

Figure 19 – Coefficients of molecular diffusivity, D_m, and coefficients of effective diffusivity, D_{ef}, expressed as a function of time for an initial concentration of OA of 50 μmol L^{-1}.

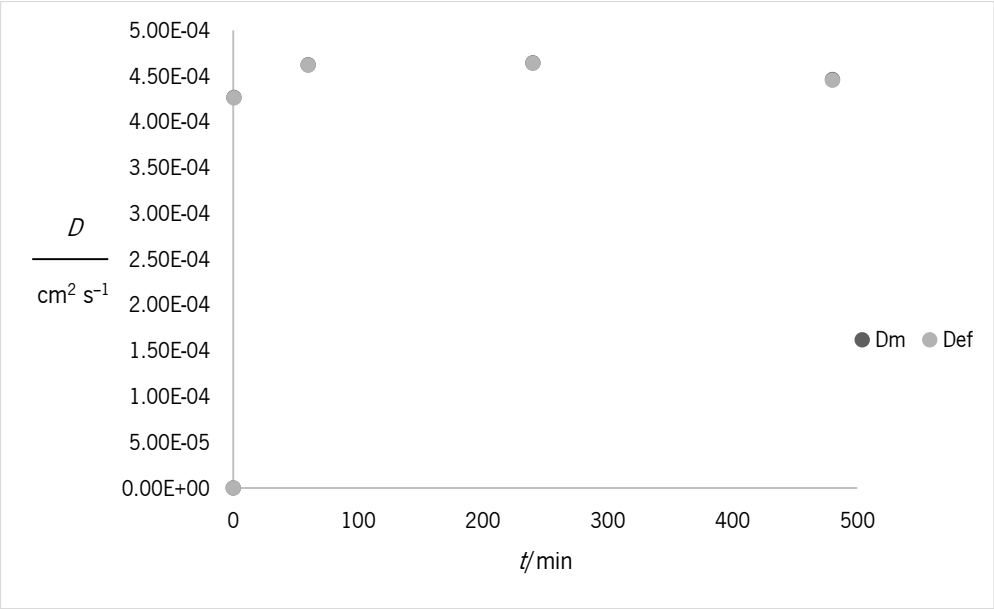

Figure 20 – Coefficients of molecular diffusivity, D_m, and coefficients of effective diffusivity, D_{ef}, expressed as a function of time for an initial concentration of OA of 100 μmol L^{-1}.

4.5. Adsorption Isotherm at 19 °C

The adsorption isotherm at 19 °C was obtained by plotting the OA mass absorbed in equilibrium, q_e, against the concentration of OA in solution at equilibrium, C_e, as shown in Figure 21. The isotherm has a linear shape. The quantity absorbed in equilibrium is given by the adsorption kinetics. The Freundlich adsorption isotherm is represented in Figure 22. This isothermal is described by the equation 1. The equation of the isotherm was obtained by a linearization of that same equation, which is $\lg q_e = \lg K_F + \left(\frac{1}{n}\right) \times \lg C_e$. In this equation $\lg K_F$ is the intercept and $\frac{1}{n}$ represents the slope. The linear shape was expected since the concentrations of OA in equilibrium are very low. The values of K_F, $1/n$, n, and R^2 are described in Table 3, and were obtained by linear regression of experimental values. The error was obtained by the regression as well.

The isotherm linearization equation is: $\lg q_e = (0.578 \pm 0.089) \lg C_e + (4.344 \pm 0.049)$.

The isotherm equation is: $q_e = (22\,085 \pm 0.049) \times C_e^{(0.578 \pm 0.089)}$.

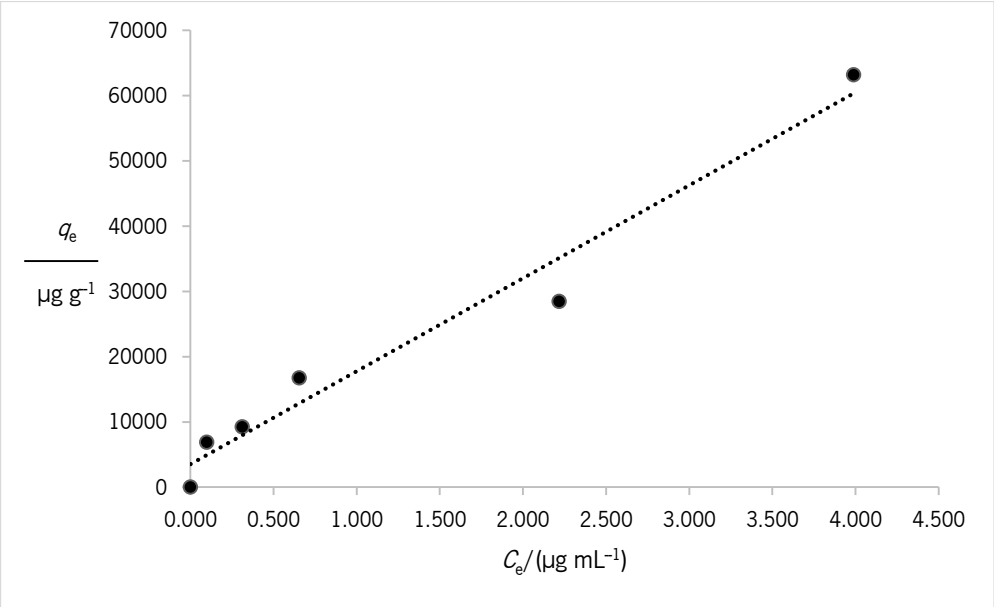

Figure 21 – Quantity of OA adsorbed in equilibrium, q_e, as a function of OA concentration in solution in equilibrium, C_e (R^2 = 0.967).

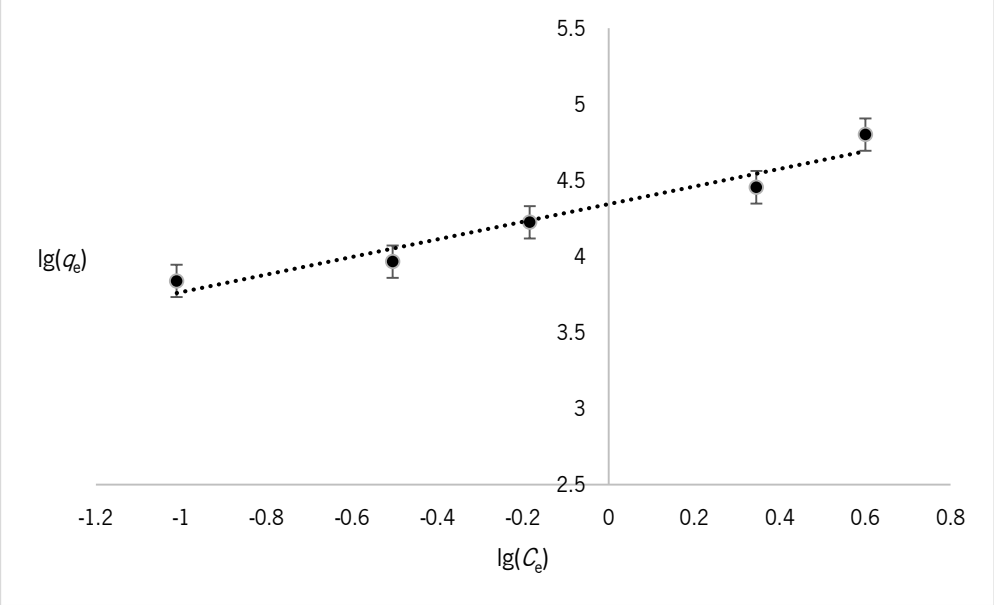

Figure 22 – Linear Regression for the Freundlich Isotherm.

Table 3 – Isotherm equation constants and correlation coefficient of the linearization

K_F	22 085 ± 0.05
$1/n$	0.578 ± 0.089
n	1.729
R^2	0.924

4.6. Recycling Tests

The results of recycling tests are shown in Figures 23 (adsorption) and 24 (desorption). Recycling tests were made for three adsorptions/desorption cycles. Figure 23 shows, that after the three cycles, *PC* values are very high: more than 80 % in the first two uses and slightly less than 80 % in the second use. Figure 24 shows that more than 50 % of OA can be recovered after the first use. This decrease in the OA recovery explains the slight decrease in adsorption capacity showed in the second use cycle (Figure 23). The error was calculated using the command DESVPAD.P of *Microsoft Excel®*.

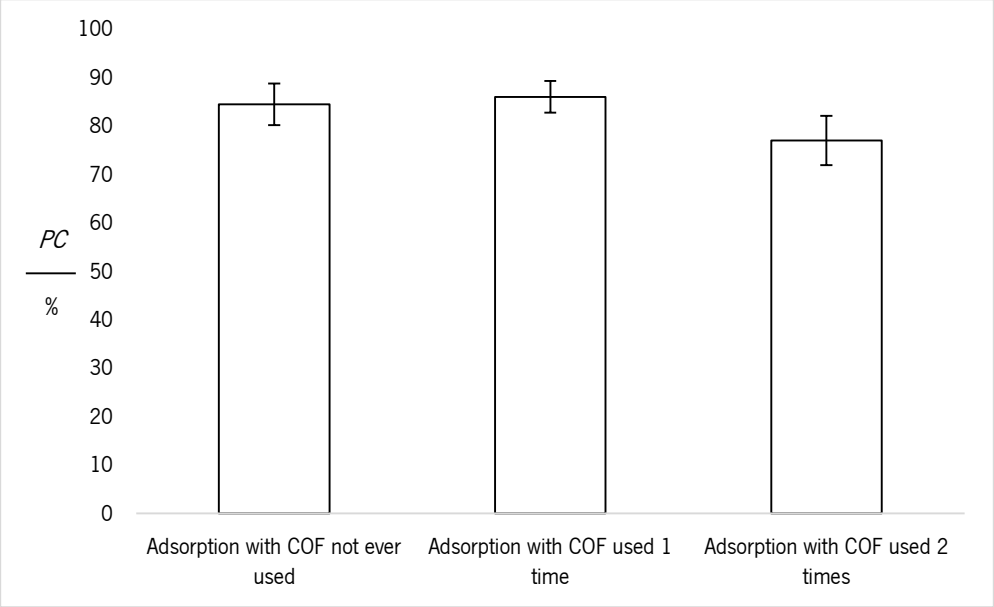

Figure 23 – Percentage of OA captured, *PC*, after three uses of the same COF.

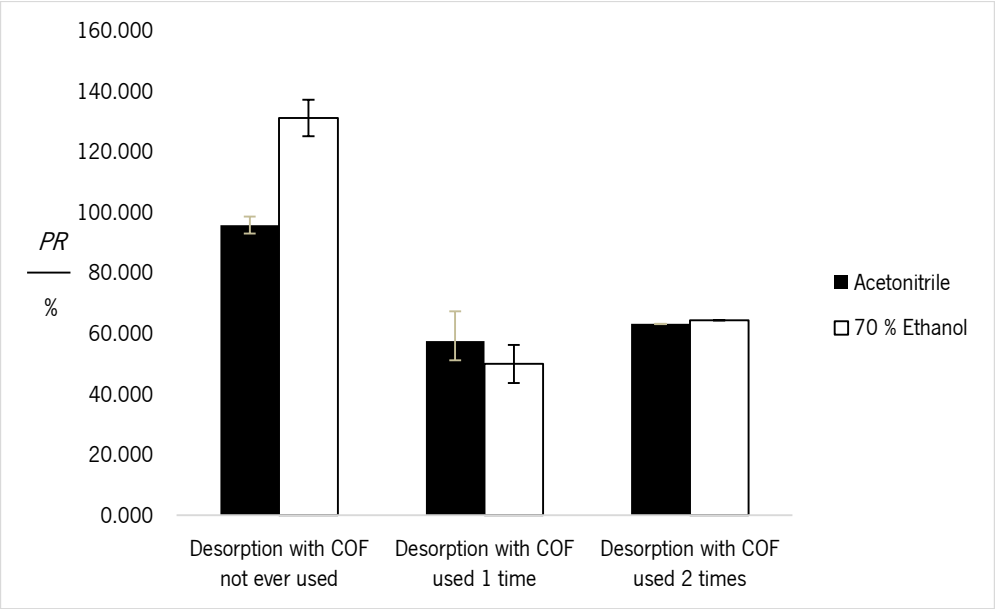

Figure 24 – Percentage of OA recovered, *PR*, after three uses of the same COF.

4.7. Mixture of Toxins Tests

Tests with mixtures of toxins were performed, however the quantification method for OA could not provide any information about the adsorption efficiency because saxitoxin interfered in the enzymatic activity of PP-1 at the tested concentrations surprisingly (Figure 25). In Figure 25 are represented a calibration curve of OA in S.W., and the red point correspond to STX positive control (c=1 µmol L^{-1}) In this way, we cannot conclude about the specificity of the COF for the OA or the possible interference of saxitoxin in its adsorption. Quantification of STX and OA will be performed by using other detection techniques (namely UPLC) out of the scope of this master thesis due to time constrains.

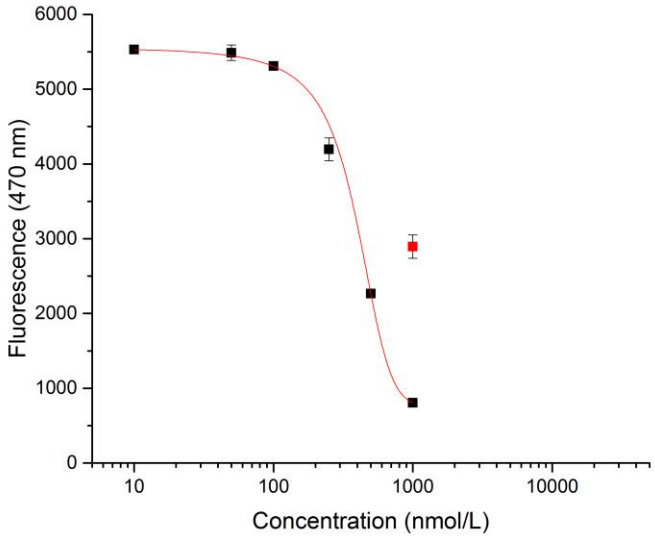

Figure 25 – Calibration curve of OA in S.W. (R^2=0.999). The red point is the point correspondent to the positive control of STX.

4.8. SPATT laboratory prototypes devices

SPATT laboratory prototype devices were fabricated and their stability in seawater was tested. In Figure 26 is shown the first SPATT device prototype. After two complete cycles of adsorption/ desorption it started leaking.

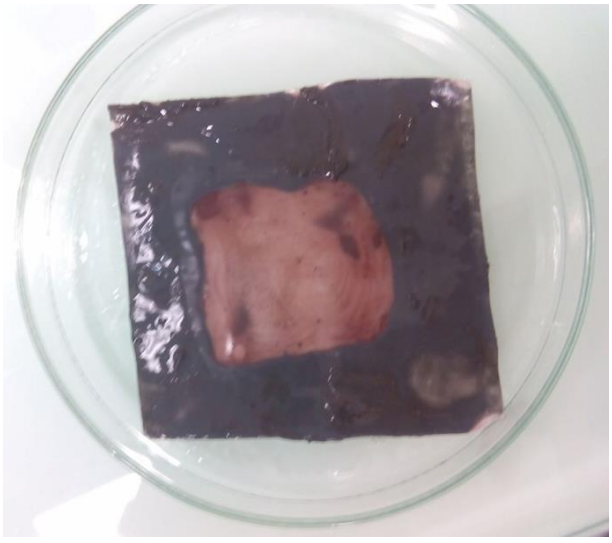

Figure 26 – SPATT device with polymeric resin.

Figure 27 shows the device fabricated with dialysis cellulose bags. This device showed no leaking for 4 cycles of adsorption/desorption. Thus, this device prototype demonstrated to be more resistant than the previous one, and easier to prepare, as well.

Figure 27 – SPATT made with dialysis bags.

5. Discussion of Results

The major aim of this thesis is to understand how a new nanoporous material can be used for biotoxin capture. To comprehend how it can be done, several laboratory test were made, as adsorption kinetics and reuse tests. The results obtained from these tests are discussed below.

The adsorption kinetics shown in section 4.1. follow Langergreen's Pseudo-First Order kinetic model. This model is usually used to model adsorption of a solute from a liquid solution. It has been applied to the adsorption of mixtures of pollutants from wastewater (Tseng *et al.*, 2010). This model can be applied to the experimental data obtained, which can be seen by R^2 of each curve.

The curves have an exponential phase in the first 60 minutes of adsorption reaction. This happens because in the beginning of the adsorption reaction, there is a large amount of available surface area, onto which the molecules can adsorb (Li *et al.*, 2011). As time passes by, the adsorption reaction reaches an equilibrium between adsorption and desorption due to the process dynamics. The equilibrium is traduced into a curve flattening.

As adsorption is an exothermic process, for a constant temperature it is expected that a higher initial concentration of adsorbate implies a higher quantity adsorbed (Seader and Henley, 2006). In the case of OA adsorption onto the COF, it was confirmed. When higher initial concentrations of OA were used, the quantity adsorbed by the COF was higher. The adsorption is almost instantaneous, because half a minute after the starting, the quantity of OA adsorbed is about a half of the equilibrium quantity.

Comparing the results obtained with the results from other studies about adsorption of OA using chromatographic resins (Fan *et al.*, 2014), the kinetic curves show the same behavior as the obtained adsorption kinetic curves. Fan and co-workers reported that adsorption equilibrium in the kinetic curves was reached at 225 min using HP–20 resin, when in this work equilibrium is reached at 60 min. Therefore, TpBD-Me_2 COF when used as adsorbent, is faster than other resins used in SPATT devices.

Other advantage of using COFs instead of other resins in SPATT devices for monitoring lipophilic marine biotoxins is that there is no need for an activation step of the material. Most of the resins used in SPATTs are very polar, and thus a step of activation, which consists in a wash of resins in

a lipophilic solvent, to turn the pores more lipophilic is required (Fux *et al.*, 2008). Due to the more lipophilic pore of the COF, the process of development of SPATT devices becomes easier.

The percentages of OA captured in the COF are shown in section 4.2. Since adsorption is an exothermic process, is expected that when a lower initial concentration of toxin is used, less toxins stays captured in the COF pores. The results obtained show this tendency, because at lower concentrations, a lower quantity of toxin is captured. At a concentration of 10 μmol L^{-1}, the maximum quantity adsorbed is reached. At higher initial concentrations, the tendency is to stabilize the quantity of captured OA at about 75 %. This might be explained by the fact that adsorption is a dynamic process, where the equilibrium occurs when the adsorbed quantity of adsorbate is equal to the desorbed quantity of adsorbate (FCTUC - Departamento de Engenharia Química, 2007). Variability on the adsorption capacity can be explained by several factors such as a variability in the OA quantification or presence of an unknown quantity of amorphous material among the COF, which reduces the capacity of adsorption.

In the present study the maximum of OA adsorbed experimentally observed was 60 600 μg g^{-1} when using the highest initial concentration (100 μmol L^{-1}). Li and co-workers (Li *et al.*, 2011) obtained with the resins HP-20 and SP700, for an initial concentration of 100 μg mL^{-1}, a maximum capacity of OA captured of 1 639 μg g^{-1} and 1 088 μg g^{-1}, respectively at 25 ºC by using the equation $q_m = K_F \times C_0^{1/n}$. Using this equation, COF maximum adsorption capacity (q_m) is 316.9 mg g^{-1}, which is almost two hundred times higher. Thus, COF can adsorb thirty times more OA than the best performing resin. Even considering that adsorption is favored at lower temperatures, and that our assays where performed at 19 ºC, the better performance of the COF when compared to the regular resins is demonstrated.

The maximum OA recovery by desorption of the pellets (section 4.3.) were obtained, with 70 % ethanol. However, this solvent can influence the fluorescence in the quantification method. On the other hand, pure acetonitrile seems to influence the enzymatic activity of PP-1, as it can be seen observed in calibration curves (Annex III). The differences and variability observed of PP-1 activity in the used solvents could be due to a lower sensitivity of the quantification method used, which is translate in a lower slop in calibration curves. The lower sensitivity of the method could be an influence of the solvents. In this way, the results of desorption, when the average *PR* of OA is at

least 50 %, but it can be higher This is also confirmed by the results of recycling tests: a constant *PC* of OA is obtained after three cycles, however, *PR* of OA is no more than 80 %.

These results indicate that the enzymatic method for OA quantification in the presence of organic solvents may be not the most adequate, however, as this detection method is rapid and sensitive, it can be used to have an initial idea of clean the COF pores are.

The diffusion, in this case, can be evaluated by D_m and D_{ef} only (section 4.4). This is possible because there is no tortuosity in the COF particles. The adsorbate pursues a linear trajectory towards the adsorbent. As COF is a highly porous material (ε=0.999), a 2D solids, and the tortuosity is inexistent, D_m and D_{ef} are mostly the same. The quick adsorption of the OA showed at the first point in time, where almost of half of the q_e is adsorbed is achieved, in the kinetics can justify that the barriers to diffusion are so tiny that they do not interfere in adsorption process. The adsorption process is, this way, faster and simpler than the adsorption process with others resins. In Figure 7 (Section 2.7) are represented how an analyte diffuses into a common adsorbent. As can be seen, the trajectory that the analyte pursues until the inner pores are not direct, creating, this way, difficulties to the diffusion in the pores. However, by using COF, due its constant structure and pore size, these difficulties can be override.

Therefore, in this adsorption process, the first step in liquid adsorption, external mass transfer of the solute from the bulk fluid through a thin film to the outer, solid surface of adsorbent (Seader and Henley, 2006) can be neglected. On the other hand, these barriers are a reality in other resins, because of their pore distribution, and irregularities in their surface (Fux *et al.*, 2008; Li *et al.*, 2011). COF have a constant pore with a constant surface. As so, the diffusion can be described by D_m and D_{ef}. At last, the higher the initial concentration of OA used, the higher is the D_m and D_{ef}. However, we need to take into account that when COF would be used in SPATT devices, the barriers to diffusion will appear, because of the nylon network where the COFs will be confined. Consequently, the kinetics will be different in the device, and adsorption of toxins will be slower when compared with lab-scale tests where COFs are not confined and are in direct contact with the toxin.

The adsorption isotherm was carried out at 19 °C (section 4.5.), because the major of DSP cases happen in waters of the regions of the planet with temperate climates, so the water in these regions should not be hotter than 20 °C. In liquid adsorption, when the binary mixture is in the dilute

region, only the solute will adsorb, and there is no interference of the solvent. In these cases, the shape of the adsorption isotherm resembles the shape obtained with pure gases. In these cases it is common to apply the Langmuir equation or the Freundlich equation (Seader and Henley, 2006). In this work, the liquid mixture can be included in the dilute region because the concentrations of OA used in the adsorption assays are in the order of 10^{-6} mole per liter. In this way, the models mentioned above can be applied.

Langmuir isotherm (equation 2) presupposes that adsorbent surface is homogeneous, every active site has the same affinity to the solute, and that there is no interaction between the adsorbed molecules. It also assumes that a monolayer of solute molecules is formed and that adsorption is a reversible process (FCTUC - Departamento de Engenharia Química, 2007). When this model was applied to the experimental data obtained in this work, the error squared was very high, and thus, the model was not suitable for this data.

The Freundlich model (equation 1) is an adequate model to describe adsorption onto heterogeneous surfaces and in low ranges of initial concentration of solute. This model was suitable to experimental data obtained. The constant n of the model, the parameter that reflects the degree of heterogeneity of the surface, is higher than 1, making the isotherm favorable (FCTUC - Departamento de Engenharia Química, 2007). The constant n is also related with the distribution of bond strengths among the surface sites. The higher the difference between n and the unit, the higher the distribution of the bond energies (Apak, 2002). In this work, as n obtained is higher than one, the isotherm is favorable. The n value obtained is also near 1. Thus, the distribution of bond energies in each pore of the adsorbent surface is very constant.

K_F is an indicator of adsorption capacity, so the higher is the value of K_F the higher the maximum adsorption capacity. This constant decreases with increasing temperature (Seader & Henley, 2006). It is also related to the strength of adsorbate–sorbent interaction (Apak, 2002). In this study, the high adsorption capacity of the COF is demonstrated also in the adsorption kinetics, so that a high value of K_F was expected. When compared the K_F value obtained by Li an co-workers (Li *et al.*, 2011), we obtained a much higher (about 800 times higher), which corroborate that the studied COF is a better adsorbent than HP-20.

The linear shape of the isotherm indicates that it can be a linear or the range of concentrations tested are in the exponential part of a favorable isotherm. The linear shape of isotherm shows that

adsorbed quantity is proportional to the equilibrium concentration of the solute in the solution, but it does not show the maximum of the capacity for the adsorption.

A linear isotherm is typically a characteristic of a homogeneous adsorbent surfaces and occurs at a low concentration (FCTUC - Departamento de Engenharia Química, 2007). The linear shape is also an indicator that all the pores have the same affinity to OA (Li *et al.*, 2011). Thus, there is no rearranging processes due to the constant pore size, and the same affinity to OA in every pore, which makes adsorption in the COF almost ideal.

However, since the experimental data are in the dilute region, there is no certainty that the linearity of the isotherm remains when higher concentrations of OA are used. Adsorption with higher concentrations will help to elucidate this, however, the scarcity and cost of the OA standard toxin made this impossible to attain in this study.

Recycling tests not only proved the reusability of the TpBD-Me_2 COF as adsorbent of OA, but also corroborates their stability, which was expected, not only in sea water, but also in organic solvents (70 % ethanol and pure acetonitrile). Although the desorption results are not so constants, the results of adsorption assays are very constants. The *PC* of OA values are practically the same, if the error is taken in account. In this line of thought, it can be affirmed that organic solvents interfere with enzymatic method of detection of OA proposed by Vieytes and co-workers, in 1997 (Vieytes *et al.*, 1997).

In any case, these results show that the COF in study can be reused for the adsorption of lipophilic marine toxins at least three times. Additionally, the capacity of adsorption does not decrease, if there is no loss of adsorbent material.

Saxitoxin is a toxin known as a PSP toxin produced by marine dinoflagellates and cyanobacteria, in freshwater environments, and, when shellfish contaminated is consumed, could be fatal (1 mg is enough to kill). It is a very polar molecule, hydrophilic and much smaller than OA (Wiese *et al.*, 2010). Due to those differences between the two molecules we selected this toxin to check both the COF preference for lipophilic small molecules and the possible interference of a small molecule that could co-occur together with OA at similar concentrations in seawater. Theoretically, as TpBD-Me_2 COF has a lipophilic pore due its methyl groups in the pore itself, STX, as a polar molecule, should not adsorb. However, with the enzymatic method of quantification, however, this toxin seems to interfere with the enzymatic method of quantification of OA so no conclusion about how

STX interfere in OA adsorption in this COF can be made so far. Despite of being interesting, how saxitoxin interfere with PP-1 or its substrate (DiFMUP), and inhibits it, was not studied, but this should be taken into account when using natural samples.

SPATT laboratory prototype devices showed some difficulties in their construction. First, a microparticule material as COFs has the tendency to be susceptible to static electricity. Due their low density, they are hard to weight without introducing any error. Finding a material with a pore size that would be suitable to COF size and stable in S.W. was also a challenge. However, nylon mesh and dialysis bags seem adequate to confine COFs and resilient to S.W. corrosive effect.

The two prototypes tested showed resistance to traction, and S.W., and for the second prototype it was demonstrated that could resist up to 4 cycles. In the future higher number of cycles would be useful so further studies will be necessary to improve the life time of SPATT devices in order to be re-used in the field.

6. Conclusions and Recommendations

In this work the main aim, checking if the innovative mesoporous group of materials named COFs, in particularly the TpBD-Me_2 COF, can be used to capture marine toxins from water, was achieved. Lipophilic toxins, such as OA, are captured and retained in the COF pores.

Our laboratory tests also proved that the COF in study can adsorb OA four times faster, and thirty times more quantity of toxin than the most successfully used resins in SPATT devices so far, HP-20. On the other hand, as COFs' pores are already lipophilic, the activation step, necessary when other resins are used as toxin adsorbents, can be dismissed. All together make that the studied COF can be an ideal candidate as adsorbent to replace usual resins in SPATT devices.

At laboratory scale, COFs were proved, due their constant structure and constant pore distribution, not to have measurable barriers to diffusion of OA. Kinetic studies showed that, at the temperature of 19 ºC, adsorption of OA is practically instantaneous. However, when COF would be used in SPATT devices, barriers to diffusion, COF physical container, where the nanoporous material will be confined, will be a reality. In this way, it is recommended that adsorption studies with COF confined will be made to understand how that barriers can influence the adsorption. Conversely, those barriers could be minimized if COF could be immobilized onto a surface, one matter of further research.

The isotherm, obtained at 19 ºC, is linear and it's a favorable one. This means that, at the range of tested concentrations, which is low, maximum adsorption capacity cannot be reached. With the obtained isotherm we can also conclude that COF have a very homogenous surface of adsorption. However, as the range of concentrations tested is low, it is recommended that studies with higher concentrations and other temperatures will be performed to completely evaluate the isotherm behavior.

To sum up, this study proves that the studied COF are effective adsorbents for lipophilic marine toxins, and, when applied to SPATT devices, can be used to provide an early warning about high concentrations of this toxins, avoiding this way that shellfish become toxic and improper for human consumption.

Finally, as when HAB happen not only lipophilic toxins are produced by microalgae, the influence of other toxins in the adsorption should be studied. On the other hand, COFs with hydrophilic or

functionalized pores should also be tested in other to get more selectivity in adsorption and to attain the most complete HABs monitoring devices.

REFERENCES

Anderson, D. M. (2009). Approaches to monitoring, control and management of harmful algal blooms (HABs). *Ocean & Coastal Management*, 52(7), 342–347. http://doi.org/10.1016/j.ocecoaman.2009.04.006

Apak, R. (2002). Adsorption of Heavy metal ions on soil surfaces and similar substances. In A. T. Hubband (Ed.), *Encyclopedia of Surface and Colloid Science -, Volume* 1 (pp. 385–417). New York: Marcel Dekker, Inc.

Backer, L. C., & Mcgillicuddy, D. J. J. (2006). Harmful Algal Blooms. *Oceanography*, 19(2), 94–106. http://doi.org/10.1016/0140-6736(93)92085-8

Barros, M. A. S. D., Arroyo, P. A., & Silva, E. A. (2013). General Aspects of Aqueous Sorption Process in Fixed Beds. In H. Nakajima (Ed.), *Mass Transfer - Advances in Sustainable Energy and Environment Oriented Numerical Modeling* (pp. 361–386). InTech. http://doi.org/10.5772/51954

Carvalho, T. E. M. de, Fungaro, D. A., & Izidoro, J. de C. (2010). Adsorção do Corante Reativo Laranja 16 de Soluções Aquosas por Zeólita Sintética. *Quim. Nova*, 33(2), 358–363. Retrieved from http://www.scielo.br/pdf/qn/v33n2/23.pdf

Chandra, S., Kandambeth, S., Biswal, B. P., Lukose, B., Kunjir, S. M., Chaudhary, M., ... Banerjee, R. (2013). Chemically stable multilayered covalent organic nanosheets from covalent organic frameworks via mechanical delamination. *Journal of the American Chemical Society*, 135(47), 17853–17861.

Côte, A. P., Benin, A. I., Ockwing, N. W., O'Keeffe, M., Matzger, A. J., & Yaghi, O. M. (2005). Porous, Crystalline, Covalent Organic Frameworks. *Science*, 310(5751), 1166–1170. http://doi.org/10.1126/science.1120411

Díaz, U., & Corma, A. (2016). Ordered covalent organic frameworks, COFs and PAFs. From preparation to application. *Coordination Chemistry Reviews*, 311, 85–124. http://doi.org/10.1016/j.ccr.2015.12.010

Ding, S.-Y., & Wang, W. (2013). Covalent organic frameworks (COFs): from design to applications. *Chem. Soc. Rev.*, 42(2), 548–568. http://doi.org/10.1039/C2CS35072F

Doucette, G. J., Mikulski, C. M., Jones, K. L., King, K. L., Greenfield, D. I., Marin, R., ... Scholin, C. A. (2009). Remote, subsurface detection of the algal toxin domoic acid onboard the Environmental Sample Processor: Assay development and field trials. *Harmful Algae*, 8(6), 880–888. http://doi.org/10.1016/j.hal.2009.04.006

Espiña, B., Louzao, Mc., Cagide, E., Alfonso, A., Vieytes, M. R., Yasumoto, T., & Botana, L. M. (2010). The methyl ester of okadaic acid is more potent than okadaic acid in disrupting the actin cytoskeleton and metabolism of primary cultured hepatocytes. *British Journal of Pharmacology*, 159(2), 337–344. http://doi.org/10.1111/j.1476-5381.2009.00512.x

Espiña, B., Prado, M., Vial, S., Martins, V. C., Rivas, J., & Freitas, P. P. (2015). New techniques in environment monitoring. In L. M. Botana, M. C. Louzao, & N. Vilariño (Eds.), *Climate Change and Marine and Freshwater Toxins* (1st ed., pp. 35–98). Berlin: De Gruyter.

European Commission. Commission Regulation (EC) No 2074/2005 of 5 December 2005 laying down implementing measures for certain products under Regulation (EC) No 853/2004 of the European Parliament and of the Council and for the organisation of official controls under Regulatio, L 338 Official Journal of the European Union 27–59 (2005).

European Commission. Commission Regulation (EU) No 15/2011 amending Regulation (EC) No 2074/2005 as regards recognised testintg methods for detecting marine biotoxins in live bivalves molluscs, L 6 Official Journal of the European Union 3–6 (2011).

European Food Safety Authority. (2008). Opinion of the Scientific Panel on Contaminants in the Food chain on a request from the European Commission on marine biotoxins in shellfish – okadaic acid and analogues. *The EFSA Journal*, 589, 1–62. Retrieved from http://www.efsa.europa.eu/sites/default/files/scientific_output/files/main_documents/589.pdf

European Parliament, & Council of European Union. Regulation (EC) No 853/2004 laying down specific hygiene rules for food of animal origin, L 139 Official Journal of the European Union 55 (2004).

Fan, L., Sun, G., Qiu, J., Ma, Q., Hess, P., & Li, A. (2014). Effect of seawater salinity on pore-size distribution on a poly(styrene)-based HP20 resin and its adsorption of diarrhetic shellfish toxins. *Journal of Chromatography A*, 1373, 1–8. http://doi.org/10.1016/j.chroma.2014.11.008

FAO. (2004). Marine Biotoxins. *FAO Food and Nutrition*. Retrieved from http://www.fao.org/docrep/007/y5486e/y5486e0e.htm#TopOfPage

FCTUC - Departamento de Engenharia Química. (2007). Adsorção e Permuta Iónica. Retrieved June 27, 2016, from http://labvirtual.eq.uc.pt/siteJoomla/index.php?option=com_content&task=view&id=188&Itemid=450

Feng, X., Ding, X., & Jiang, D. (2012). Covalent organic frameworks. *Chem Soc Rev*, 41(18), 6010–22. http://doi.org/10.1039/c2cs35157a

Fux, E., Marcaillou, C., Mondeguer, F., Bire, R., & Hess, P. (2008). Field and mesocosm trials on passive sampling for the study of adsorption and desorption behaviour of lipophilic toxins with a focus on OA and DTX1. *Harmful Algae*, 7(5), 574–583. http://doi.org/10.1016/j.hal.2007.12.008

Garibo, D., Dàmaso, E., Eixarch, H., de la Iglesia, P., Fernández-Tejedor, M., Diogène, J., ... Campàs, M. (2012). Protein phosphatase inhibition assays for okadaic acid detection in shellfish: Matrix effects, applicability and comparison with LC–MS/MS analysis. *Harmful Algae*, *19*(2012), 68–75. http://doi.org/10.1016/j.hal.2012.06.001

Gilbert, P. M., Anderson, D. M., Gentien, P., Granéli, E., & Sellner, K. G. (2005). The Global Complex Phenomena of Harmful Algal Blooms. *Oceanography*, 18(2), 130–141. http://doi.org/http://dx.doi.org/10.5670/oceanog.2005.49

Greenfield, D. I., Marin, R., Doucette, G. J., Mikulski, C., Jones, K., Jensen, S., ... Scholin, C. (2008). Field applications of the second-generation Environmental Sample Processor (ESP) for remote detection of harmful algae: 2006-2007. *Limnology and Oceanography: Methods*, 6(12), 667–679. http://doi.org/10.4319/lom.2008.6.667

Han, M. Y., & Kim, W. (2001). A theoretical consideration of algae removal with clays. *Microchemical Journal*, 68(2-3), 157–161. http://doi.org/10.1016/S0026-265X(00)00142-9

Hosoi-Tanabe, S., & Sako, Y. (2005). Rapid detection of natural cells of Alexandrium tamarense and A. catenella (Dinophyceae) by fluorescence in situ hybridization. *Harmful Algae*, 4(2), 319–328. http://doi.org/10.1016/j.hal.2004.04.002

Jewett, E. B., Lopez, C. B., Dortch, Q., Etheridge, S. ., & Backer, L. C. (2008). *Harmful Algal*

Bloom Management and Response: Assessment and Plan. Interagency Working Group on Harmful Algal Blooms, Hypoxia, and Human Health of the Joint Subcommittee on Ocean Science and Technology Washington, DC.

Lawley, R. (2013). Okadaic Acid Toxins. Retrieved March 14, 2016, from http://www.foodsafetywatch.org/factsheets/okadaic-acid-toxins/

Li, A., Ma, F., Song, X., & Yu, R. (2011). Dynamic adsorption of diarrhetic shellfish poisoning (DSP) toxins in passive sampling relates to pore size distribution of aromatic adsorbent. *Journal of Chromatography. A*, 1218(11), 1437–42. http://doi.org/10.1016/j.chroma.2011.01.043

Lloyd, J. K., Duchin, J. S., Borchert, J., Quintana, H. F., & Robertson, A. (2013). Diarrhetic Shellfish Poisoning, Washington, USA, 2011. *Emerging Infectious Diseases*, 19(8), 1314–1316. http://doi.org/10.3201/eid1908.121824

MacKenzie, L. A. (2010). In situ passive solid-phase adsorption of micro-algal biotoxins as a monitoring tool. *Current Opinion in Biotechnology*, 21(3), 326–331. http://doi.org/10.1016/j.copbio.2010.01.013

MacKenzie, L., Beuzenberg, V., Holland, P., McNabb, P., & Selwood, A. (2004). Solid phase adsorption toxin tracking (SPATT): a new monitoring tool that simulates the biotoxin contamination of filter feeding bivalves. *Toxicon : Official Journal of the International Society on Toxinology*, 44(8), 901–18. http://doi.org/10.1016/j.toxicon.2004.08.020

McCarthy, M., van Pelt, F. N. A. M., Bane, V., O'Halloran, J., & Furey, A. (2014). Application of passive (SPATT) and active sampling methods in the profiling and monitoring of marine biotoxins. *Toxicon*, 89, 77–86. http://doi.org/10.1016/j.toxicon.2014.07.005

McNabb, P. (2008). Chemistry, Metabolism and Analysis of Okadaic Acid Group. In L. M. Botana (Ed.), *Seafood and Freshwater Toxins: Pharmacology, Physiology and Detection* (2nd ed., pp. 209–228). CRC Press.

National Centers for Coastal Ocean Science. (2016). Phytoplankton Monitoring Network. Retrieved April 4, 2016, from https://coastalscience.noaa.gov/research/habs/pmn

National Oceanic and Atmspheric Administration. (2016). Harmful Algal Blooms. Retrieved March 4, 2016, from http://oceanservice.noaa.gov/hazards/hab/

Pharmacelsus. (2015). IC50 Determination. Retrieved March 17, 2016, from http://www.pharmacelsus.de/ic50/

Prego-Faraldo, M. V., Valdiglesias, V., Méndez, J., & Eirín-López, J. M. (2013). Okadaic acid meet and greet: an insight into detection methods, response strategies and genotoxic effects in marine invertebrates. *Marine Drugs*, 11(8), 2829–45. http://doi.org/10.3390/md11082829

Qiu, H., Lv, L., Pan, B., Zhang, Q., Zhang, W., & Zhang, Q. (2009). Critical review in adsorption kinetic models. *Journal of Zhejiang University SCIENCE A*, 10(5), 716–724. http://doi.org/10.1631/jzus.A0820524

Rundberget, T., Gustad, E., Samdal, I. A., Sandvik, M., & Miles, C. O. (2009). A convenient and cost-effective method for monitoring marine algal toxins with passive samplers. *Toxicon : Official Journal of the International Society on Toxinology*, 53(5), 543–50. http://doi.org/10.1016/j.toxicon.2009.01.010

Sassolas, A., Hayat, A., Catanante, G., & Marty, J.-L. (2013). Detection of the marine toxin okadaic acid: Assessing seafood safety. *Talanta*, 105, 306–316. http://doi.org/10.1016/j.talanta.2012.10.049

Scoging, a C. (1998). Marine biotoxins. *Symposium Series (Society for Applied Microbiology)*, *27*, 41S–50S.

Seader, J. D., & Henley, E. J. (2006). Adsorption, Ion Change, and Chromatography. In *Separation Process Principles* (2nd Editio, pp. 548–621). John Wiley & Sons, Inc.

Seltenrich, N. (2014). Keeping tabs on HABs : New Tools for Detecting, Monitoring and Preventing Harmful Algal Blooms. *Environmental Health Perspectives*, 122(8), A206–A213. http://doi.org/dx.doi.org/10.1289/ehp.122-A206

Sigma-Aldrich Co. LLC. (2016). Diaion® HP-20. Retrieved April 1, 2016, from http://www.sigmaaldrich.com/catalog/product/supelco/13607?lang=pt&region=PT

Taylor, M., McIntyre, L., Ritson, M., Stone, J., Bronson, R., Bitzikos, O., ... Team, O. (2013). Outbreak of Diarrhetic Shellfish Poisoning Associated with Mussels, British Columbia, Canada. *Marine Drugs*, 11(5), 1669–1676. http://doi.org/10.3390/md11051669

Tseng, R.-L., Wu, F.-C., & Juang, R.-S. (2010). Characteristics and applications of the Lagergren's first-order equation for adsorption kinetics. *Journal of the Taiwan Institute of Chemical Engineers*, 41(6), 661–669. http://doi.org/10.1016/j.jtice.2010.01.014

Tubaro, A., Sosa, S., Bornancin, A., & Hungerford, J. (2008). Pharmacology and Toxicology of Diarreheic Shellfish Toxins. In L. M. Botana (Ed.), *Seafood and Freshwater Toxins: Pharmacology, Physiology and Detection* (2nd ed., pp. 229–253). CRC Press.

Turrell, E., Stobo, L., Lacaze, J.-P., Bresnan, E., & Gowland, D. (2007). Development of an `early warning system' for harmful algal blooms using solid-phase adsorption toxin tracking (SPATT). In *OCEANS 2007 - Europe* (pp. 1–6). IEEE. http://doi.org/10.1109/OCEANSE.2007.4302436

United States Environmental Protection Agency. (2016a). Climate Change and Harmful Algal Blooms. Retrieved March 4, 2016, from http://www.epa.gov/nutrientpollution/climate-change-and-harmful-algal-blooms

United States Environmental Protection Agency. (2016b). Harmful Algal Blooms. Retrieved March 4, 2016, from http://www.epa.gov/nutrientpollution/harmful-algal-blooms

Vermeulen, T., LeVan, M. D., Hiester, N. K., & Klein, G. (1984). Adsorption and Ion Exchange. In R. H. Perry, D. W. Green, & J. O. Maloney (Eds.), *Perry's Chemical Engineers' Handbook* (6th Editio, pp. 16–1–16–48). Singapore: McGraw-Hill International Editions.

Vieytes, M. R., Fontal, O. I., Leira, F., Baptista de Sousa, J. M., & Botana, L. M. (1997). A fluorescent microplate assay for diarrheic shellfish toxins. *Analytical Biochemistry*, 248(2), 258–64. http://doi.org/10.1006/abio.1999.3099

Wiese, M., D'Agostino, P. M., Mihali, T. K., Moffitt, M. C., & Neilan, B. A. (2010). Neurotoxic Alkaloids: Saxitoxin and Its Analogs. *Marine Drugs*, 8(7), 2185–2211. http://doi.org/10.3390/md8072185

Zendong, Z., Herrenknecht, C., Abadie, E., Brissard, C., Tixier, C., Mondeguer, F., ... Hess, P. (2014). Extended evaluation of polymeric and lipophilic sorbents for passive sampling of marine toxins. *Toxicon*, 91, 57–68. http://doi.org/10.1016/j.toxicon.2014.03.010

Zingone, A., & Oksfeldt Enevoldsen, H. (2000). The diversity of harmful algal blooms: A challenge for science and management. *Ocean and Coastal Management*, 43(8-9), 725–748. http://doi.org/10.1016/S0964-5691(00)00056-9

ANNEX I – TPBD-ME$_2$ COF POROSITY AND X-RAY DIFFRACTION PATTERN BY SMALL ANGLE X-RAY SPECTROSCOPY

The BET adsorption/desorption isotherm the performed with N_2 to calculate TpBD-Me$_2$ COF surface area and its half pore size is represented in Figure 28.

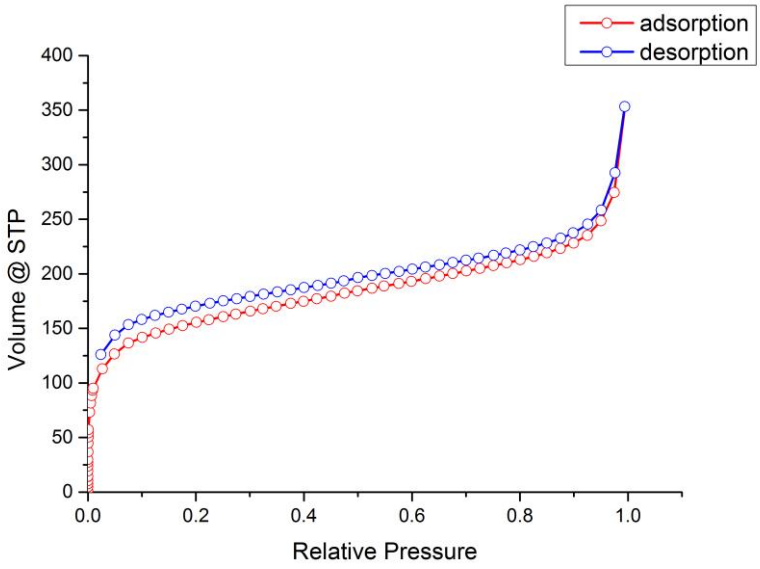

Figure 28 – BET adsorption/desorption isotherm.

Based on that data BET surface area (572.791 m^2 g^{-1}) and average of half pore size (0.60 nm) where calculated.

Small Angle X-Ray Spectroscopy (SAXS) data obtained for TpBD-Me_2 COF is shown in Figure 29. This graphic gives the information about the crystallinity of COF sample, which is traduced by the peaks.

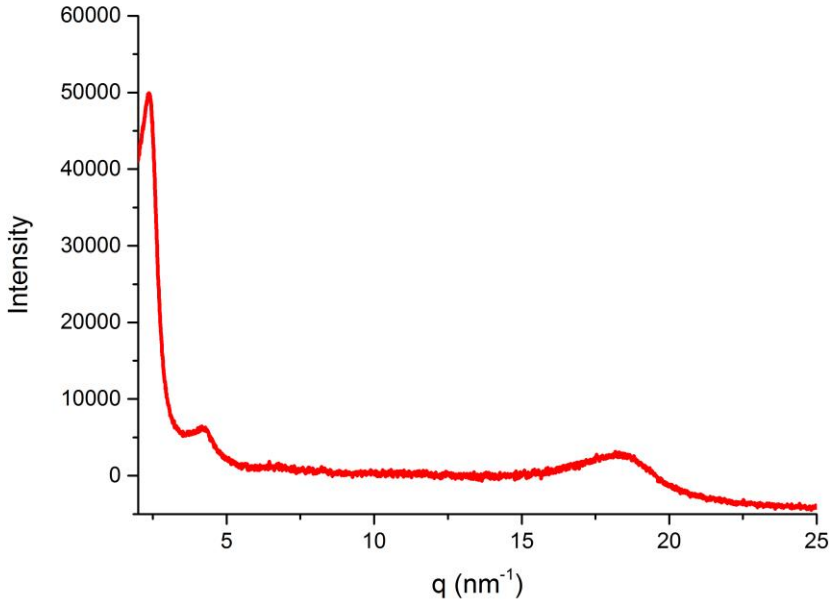

Figure 29 – X-Ray Diffraction pattern of a TpBD–Me_2 COF sample.

ANNEX II – SERIAL DILUTIONS FOR OA CALIBRATION CURVE

The OA quantification assay required a calibration curve every time it was performed. To calculate the necessary volumes to do the serial dilutions the expression $c_i \times v_i = c_f \times v_f$ were applied. The serial dilutions were made for adsorption assay in Sea Water (S.W.) and for desorption assays with 70 % ethanol or acetonitrile. An example of how the calculation of the serial dilutions in S.W. used to do the calibration curve is below.

$$100 \ \frac{\text{nmol}}{\text{L}} \times 70 \ \mu\text{L} = 500 \ \frac{\text{nmol}}{\text{L}} \times v_i \Rightarrow v_i = 14 \ \mu\text{L}$$

$$500 \ \frac{\text{nmol}}{\text{L}} \times (70+14) \ \mu\text{L} = 1\,000 \ \frac{\text{nmol}}{\text{L}} \times v_i \Rightarrow v_i = 42 \ \mu\text{L}$$

$$1\,000 \ \frac{\text{nmol}}{\text{L}} \times (70 + 42) \ \mu\text{L} = 1\,500 \ \frac{\text{nmol}}{\text{L}} = 74.7 \ \mu\text{L}$$

$$1\,500 \ \frac{\text{nmol}}{\text{L}} \times (70 + 74.7) \ \mu\text{L} = 2\,500 \ \frac{\text{nmol}}{\text{L}} \times v_i \Rightarrow v_i = 86.8 \ \mu\text{L}$$

$$2\,500 \ \frac{\text{nmol}}{\text{L}} \times (70 + 86.8) \ \mu\text{L} = 5\,000 \ \frac{\text{nmol}}{\text{L}} \times v_i \Rightarrow v_i = 78.4 \ \mu\text{L}$$

$$5\,000 \ \frac{\text{nmol}}{\text{L}} \times (70 + 78.4) \ \mu\text{L} = 10\,000 \ \frac{\text{nmol}}{\text{L}} \times v_i \Rightarrow v_i = 74.2 \ \mu\text{L}$$

$$10\,000 \ \frac{\text{nmol}}{\text{L}} \times (70 + 74.2) \ \mu\text{L} = 50\,0000 \ \frac{\text{nmol}}{\text{L}} \times v_i \Rightarrow v_i = 28.8 \ \mu\text{L}$$

$$50\,000 \ \frac{\text{nmol}}{\text{L}} \times (70 + 28.8) \ \mu\text{L} = 1\,000\,000 \ \frac{\text{nmol}}{\text{L}} \times v_i \Rightarrow v_i = 4.942 \ \mu\text{L}$$

The composition of the serial dilutions and respective concentration in the well of the microplate is below:

OA0 ($c = 5\,000 \ \frac{\text{nmol}}{\text{L}}$): 5 µL s. s. + 100 µL S.W.

OA1 ($c = 1\,000 \ \frac{\text{nmol}}{\text{L}}$): 28.8 µL OA0 + 115.4 µL S.W.

OA2 ($c = 500 \ \frac{\text{nmol}}{\text{L}}$): 74.2 µL OA1 + 74.2 µL S.W.

OA3 ($c = 250 \ \frac{\text{nmol}}{\text{L}}$): 78.4 µL OA2 + 78.4 µL S.W.

OA4 ($c = 150\ \frac{\text{nmol}}{\text{L}}$): 86.8 µL OA3 + 58 µL S.W.

OA5 ($c = 100\ \frac{\text{nmol}}{\text{L}}$): 74.8 µL OA4 + 37.4 µL S.W.

OA6 ($c = 50\ \frac{\text{nmol}}{\text{L}}$): 42 µL OA5. + 42 µL S.W.

OA7 ($c = 10\ \frac{\text{nmol}}{\text{L}}$): 14 µL OA6. + 56 µL S.W.

ANNEX III – OA CALIBRATION CURVES

Calibration curves were made using the software *OriginPro®* by plotting the known concentrations of serial dilutions against the respective fluorescence read at 470 nm. Then, a non-linear pharmacology dose-response fitting was applied. Calibration curves were made using SW, 70 % ethanol, and acetonitrile. Below are three examples of calibration curves made for each of the used solvents.

A) Calibration Curve in Sea Water

Calibration curve in S.W. and respective statistic table made for quantification assay are represented in Figure 30 and Table 4, respectively.

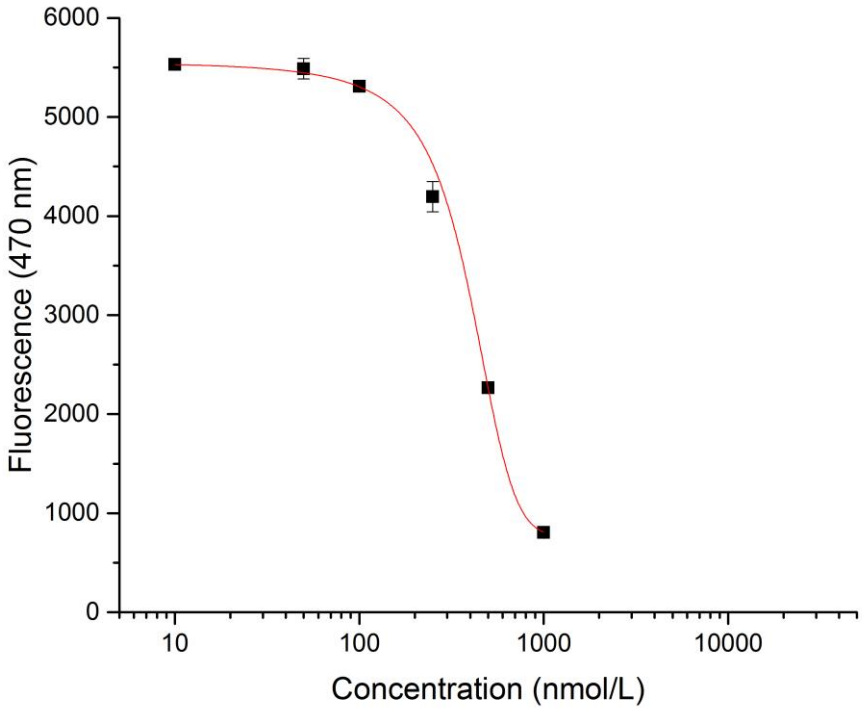

Figure 30 – OA calibration curve in seawater.

Table 4 – Statistic data from Calibration curve represented in Figure 30

Model	DoseResp
Equation	y = A1 + (A2-A1)/(1 + 10^((LOGx0-x)*p))
Plot	Fluorescence Average
A1	1116.91513 ± 151.86126
A2	5982.79425 ± 812.9893
LOGx0	439.03608 ± 201.01954
P	-0.00502 ± 0.01535
Reduced Chi-Sqr	5.24245
R-Square(COD)	0.99878
Adj. R-Square	0.99514

B) Calibration Curve in Acetonitrile

Calibration curve in acetonitrile and respective statistic table made for quantification assay are represented in Figure 31 and Table 5, respectively.

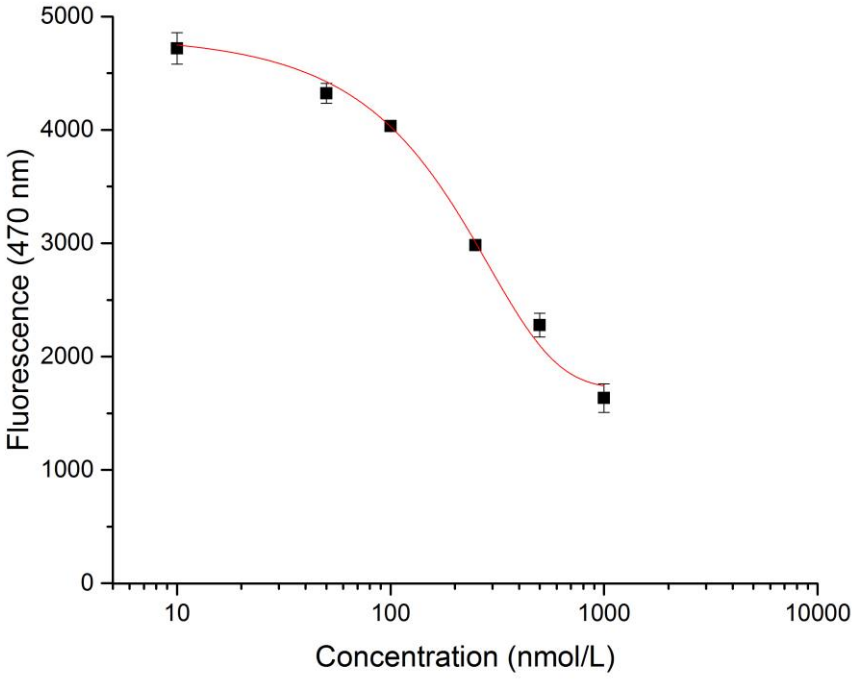

Figure 31 – OA calibration curve in acetonitrile

Table 5 – Statistic data from Calibration curve represented in Figure 31

Model	DoseResp
Equation	y = A1 + (A2-A1)/(1 + 10^((LOGx0-x)*p))
Plot	Fluorescence
A1	1718.14942 ± 225.18601
A2	7462.22564 ± 3744.79139
LOGx0	29.64319 ± 211.11799
P	-0.00244 ± 9.03533E-4
Reduced Chi-Sqr	2.8882
R-Square(COD)	0.99613
Adj. R-Square	0.99032

C) Calibration Curve in 70 % Ethanol

Calibration curve in 70 % ethanol and respective statistic table made for quantification assay are represented in Figure 32 and Table 6, respectively.

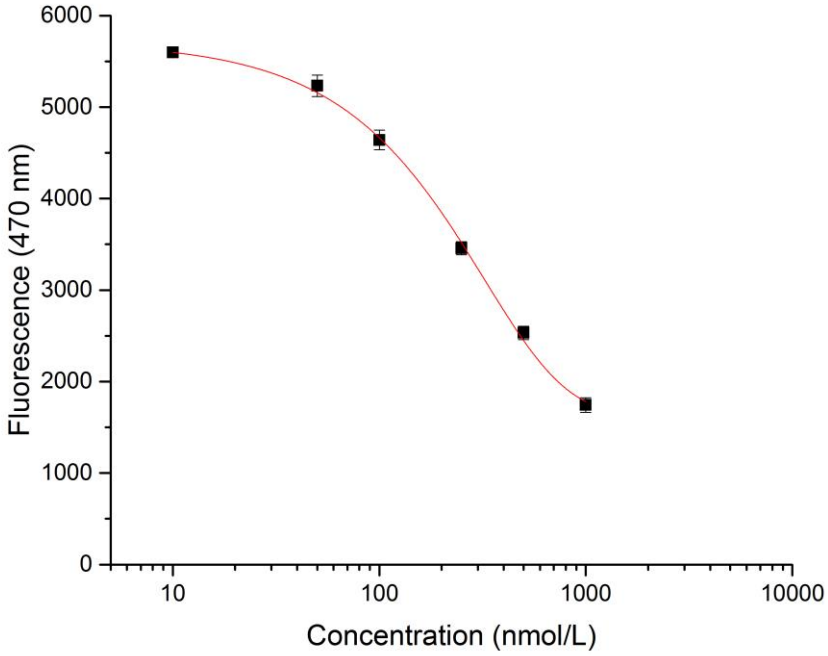

Figure 32 – OA Calibration curve in 70 % ethanol.

Table 6 – Statistic data from Calibration curve represented in Figure 32

Model	DoseResp
Equation	y = A1 + (A2-A1)/(1 + 10^((LOGx0-x)*p))
Plot	Fluorescence
A1	1645.24415 ± 175.77444
A2	21937.30366 ± 35893.87384
LOGx0	-382.87106 ± 723.62462
p	-0.00157 ± 5.07508E-4
Reduced Chi-Sqr	1.36461
R-Square(COD)	0.99947
Adj. R-Square	0.99868